THE JOURNAL OF COMPARATIVE NEUROLOGY 463:177–195 (2003)

Ultrastructural Analysis of [^{3}H]Thymidine-Labeled Cells in the Rat Utricular Macula

ELIZABETH C. OESTERLE,[1,2]* DALE E. CUNNINGHAM,[1,2]
LESNICK E. WESTRUM,[2,3] AND EDWIN W RUBEL[1,2]
[1]Department of Otolaryngology-Head and Neck Surgery, University of Washington, Seattle, Washington 98195
[2]Virginia Merrill Bloedel Hearing Research Center, University of Washington, Seattle, Washington 98195
[3]Departments of Neurosurgery and Biological Structure, University of Washington, Seattle, Washington 98195

ABSTRACT

Ototoxic drugs stimulate cell proliferation in adult rat vestibular sensory epithelia, as does the infusion of transforming growth factor alpha (TGFα) plus insulin. We sought to determine whether new hair cells can be regenerated by means of a mitotic pathway. Previously, studies have shown that the nuclei of some newly generated cells are located in the lumenal half of the sensory epithelium, suggesting that some may be newly generated sensory hair cells. The aim of this study was to examine the ultrastructural characteristics of newly proliferated cells after TGFα stimulation and/or aminoglycoside damage in the utricular sensory epithelium of the adult rat. The cell proliferation marker tritiated-thymidine was infused, with or without TGFα plus insulin, into the inner ears of normal or aminoglycoside-damaged rats for 3 or 7 days by means of osmotic pumps. Autoradiographic techniques and light microscopy were used to identify cells synthesizing DNA. Sections with labeled cells were re-embedded, processed for transmission electron microscopy, and the ultrastructural characteristics of the labeled cells were examined. The following five classes of tritiated-thymidine labeled cells were identified in the sensory epithelium: (1) labeled cells with synaptic specializations that appeared to be newly generated hair cells, (2) labeled supporting cells, (3) labeled leukocytes, (4) labeled cells that we have classified as "active cells" in that they are relatively nondescript but contain massive numbers of polyribosomes, and (5) labeled degenerating hair cells. These findings suggest that new hair cells can be generated in situ by means of a mitotic mechanism in the vestibular sensory epithelium of adult mammals. J. Comp. Neurol. 463:177–195, 2003.

Indexing terms: hair cell regeneration; vestibular; growth factor; inner ear

Inner ear hair cells are the mechanoreceptors for hearing and balance. Hair cells in the cochlea function in sound detection, whereas hair cells in the vestibular sensory epithelia detect head movements. Hair cells are vulnerable to various agents, including loud sounds, ototoxic drugs (e.g., aminoglycosides), and aging. In nonmammalian vertebrates, lost hair cells are replaced by means of renewed mitotic activity of progenitor cells (Corwin and Cotanche, 1988; Ryals and Rubel, 1988; Balak et al., 1990; Weisleder and Rubel, 1993; Baird et al., 1996) and/or the transdifferentiation (nonmitotic conversion) of supporting cells (Baird et al., 1993, 1996; Roberson et al., 1996; Adler and Raphael, 1996; Jones and Corwin, 1996). Lost hair

Grant sponsor: National Institutes of Health/National Institute on Deafness and Other Communication Disorders; Grant number: DC03944; Grant number: DC04661; Grant sponsor: the National Organization for Hearing Research Foundation (NOHR).

*Correspondence to: Elizabeth C. Oesterle, Virginia Merrill Bloedel Hearing Research Center, Box 357923, University of Washington, Seattle, WA 98195-7923. E-mail: oesterle@u.washington.edu

Received 9 May 2002; Revised 4 March 2003; Accepted 11 March 2003
DOI 10.1002/cne.10756
Published online the week of June 30, 2003 in Wiley InterScience (www.interscience.wiley.com).

cells are not replaced in the traumatized mammalian cochlea (Sobkowicz et al., 1992; Roberson and Rubel, 1994; Chardin and Romand, 1995), and it is unclear whether vestibular hair cells are normally replaced in rodents after damage.

Immature appearing stereociliary bundles are seen in the normal undamaged vestibular sensory epithelia of mature guinea pig and bats (Forge et al., 1993, 1998; Rubel et al., 1995; Lambert et al., 1997; Kirkegaard and Jørgensen, 2000, 2001), suggesting the de novo formation of vestibular hair cells in adult mammals. The origin of the immature bundles is controversial, as they could reflect the existence of newly generated hair cells, repair of native bundleless hair cells, or fluctuations in bundle structure (Sobkowicz et al., 1996, 1997; Zheng et al., 1999; Baird et al., 2000; Gale et al., 2000). New hair cell production in mature mammalian vestibular sensory epithelia is also debated. In animals recovering from drug insult, initial decreases in stereocilia and hair cell density in the in vivo chinchilla ampullae and guinea pig otolithic organs are followed by significant recovery (Lopez et al., 1997; Forge et al., 1998). However, the mechanisms of this recovery remain to be determined. They could arise by direct transdifferentiation of support cells (where hair cells arise directly from support cells without an intervening mitotic event; Li and Forge, 1997; Steyger et al., 1997; Forge et al., 1998), by dedifferentiation and recovery (Sobkowicz et al., 1996, 1997; Baird et al., 2000), or by regenerative proliferation from precursor cells. Damaged mammalian vestibular sensory epithelia show limited cell division after insult both in vitro (Warchol et al., 1993; Lambert, 1994; Zheng et al., 1997; Zheng and Gao, 1997) and in vivo (Rubel et al., 1995; Tanyeri et al., 1995; Li and Forge, 1997; Kuntz and Oesterle, 1998; Lopez et al., 1998; Ogata et al., 1999). The absence of labeled hair cells in drug-damaged guinea pig utricle continuously infused with a cell proliferation marker, or in gerbils given daily injections of bromodeoxyuridine (BrdU) after ototoxic damage, has led to concerns about whether proliferating sensory epithelial cells have the potential to generate new vestibular hair cells (Rubel et al., 1995; Ogata et al., 1999). On the other hand, in vivo data in drug-damaged rats, gerbils, and chinchilla demonstrate the presence of a small number of new cells (by mitotic activity) in lumenal regions of the vestibular sensory epithelium (SE) (Tanyeri et al., 1995; Kuntz and Oesterle, 1998; Ogata et al., 1999), a region typically occupied by hair cells. Yet, the location of the nucleus is not a reliable phenotypic indicator for cell type in damaged epithelia due to the disorganization of the tissue and migration of precursor cell nuclei to lumenal portions of the epithelium (Raphael, 1992; Katayama and Corwin, 1993; Tsue et al., 1994) and potential presence of proliferating leukocytes in the SE (Roberson and Rubel, 1994; Warchol, 1997; Bhave et al., 1998; Vago et al., 1998).

In our previous work (Kuntz and Oesterle, 1998), we showed that (1) infusion of transforming growth factor alpha (TGFα) plus insulin into the in vivo rat ear stimulates cell proliferation in the mature vestibular SE, (2) gentamicin alone also stimulates some cell proliferation in situ in this preparation, and (3) the nuclei of some newly generated cells are located in the lumenal half of the SE. Our goal in the present study was to determine the cell types represented by the newly generated cells that ended up in the lumenal region after ototoxic-induced damage or TGFα plus insulin infusion. In particular, we sought to determine whether some newly generated cells, whose nuclei are located in the lumenal portion of the SE, become hair cells based on ultrastructural criteria. We identified tritiated [^{3}H]thymidine-labeled cells by light microscopy, re-embedded the sections, and examined the same cells by transmission electron microscopy (TEM). By using ultrastructural characteristics, we identified five classes of [^{3}H]thymidine-labeled cells in the utricular SE: (1) labeled cells with immature, primordial synaptic specializations that appeared to be newly generated hair cells, (2) labeled supporting cells, (3) labeled leukocytes, (4) labeled cells that we classified as "active cells" in that they are relatively nondescript but contain massive numbers of polyribosomes, and (5) labeled degenerating hair cells. Preliminary accounts of portions of these data have appeared in abstract form (Oesterle et al., 2000).

MATERIALS AND METHODS

Animals

Adult male Sprague-Dawley rats (200–300 g, B&K Universal, Edmonds, WA) were implanted with mini-osmotic pumps. Experimental methods and animal care procedures were approved by the Institutional Animal Care and Use Committee (IACUC) at the University of Washington.

Growth factors

TGFα (Collaborative Biomedical Products, Bedford, MA, catalog no. 40054) was reconstituted in aqueous tritiated [^{3}H]thymidine (1 mCi/ml; 80–86 Ci/mmol; New England Nuclear Research Products, Wilmington, DE). Insulin (Sigma, St. Louis, MO, catalog no. I-1882) was reconstituted in sterile water.

Mini-osmotic pump and infusion cannula units

ALZET brain infusion kits (ALZA Corp., Palo Alto, CA) were modified for cochlear infusion. Each cannula and catheter was filled with test solution and connected to the mini-osmotic pump. Mini-osmotic pumps continuously delivered 1.0 μl of solution/hour for 3 (model 1003D) or 7 days (model 2001).

Surgical procedure for minipump implantation

Surgical procedures described in Rubel et al. (1995) and modified by Kuntz and Oesterle (1998) were used. Animals were anesthetized with intraperitoneal injections of ketamine (33 mg/kg; Aveco, Fort Dodge, IA) and xylazine (5 mg/kg; Mobay, Shawnee, KS). By using aseptic technique, the bulla was opened and a fistula was made in the basal turn of the cochlea to gain access to the scala vestibuli. The cannula tip was inserted into the hole, and Vetbond (3M Animal Care Products, St. Paul, MN) secured the cannula to the cochlea and the bulla. The catheter was tunneled under muscle and connected with the mini-osmotic pump, which was implanted in a pocket under the skin on the animal's back.

Experimental groups

Normal, undamaged animals. Tritiated-thymidine, which labels nuclei of cells passing through the S phase (DNA synthesis) of the cell cycle, was used to identify dividing cells. Tritiated-thymidine and TGFα (5 μg) plus

insulin (100 μg) were continuously infused by means of a mini-osmotic pump cannula system (ALZA Corp.) into normal rat ears for 3 (n = 9) or 7 (n = 7) days. On day 4 or 10 after pump implantation, the infused ears were fixed by intralabyrinthine perfusion with 3.5% glutaraldehyde in 0.1 M sodium-phosphate buffer. One ear of control animals (n = 12) was infused with [^{3}H]thymidine alone for the same periods of time.

Drug-damaged animals. To damage vestibular hair cells, gentamicin sulfate (0.1 mg; Elkins Sinn, Philadelphia, PA) was placed into the catheters leading from the pump to the inner ear and infused immediately before a 3-day infusion of [^{3}H]thymidine alone (n = 5) or [^{3}H]thymidine with TGFα (5 μg) plus insulin (100 μg; n = 5). Animals were killed on day 4 after pump placement, and the ears were fixed with 3.5% glutaraldehyde in 0.1M sodium-phosphate buffer.

Histologic and autoradiographic processing

Four or 10 days after osmotic pump insertion, animals were deeply anesthetized with ketamine and xylazine and the pump-cannula units were removed and examined. Animals were excluded from the study (and not included in any of the n's stated above) if there was evidence of infection, pump malfunction (catheter or cannula occlusion, pump disconnection from catheter), or dislodged cannula tip. Animals were killed with an intracardiac injection of sodium pentobarbital, and the oval windows were opened. Vestibular end organs were perfused with 3.5% glutaraldehyde in 0.1 M sodium-potassium phosphate buffer (pH 7.4), and temporal bones were immersed in cold fixative overnight. Utricles were dissected free and post-fixed in 1% OsO_4 in the same buffer for 30 minutes at room temperature. The tissues were dehydrated in a graded ethanol series and embedded in Spurr's epoxy resin (Polysciences, Warrington, PA). Serial semithin sections were cut at a thickness of 3 μm through each organ, mounted onto acid-washed, chrome-alum–subbed slides, and dipped in a 50% aqueous solution of nuclear track emulsion (Kodak NTB-2). Emulsion-coated slides were stored at 4°C for 3 to 5 days in light-tight boxes. Slides were developed in Kodak D-19 and counterstained with 0.01% toluidine blue before cover-slipping with DPX mounting medium.

Each utricle produced roughly 200 (3 μm) serial transverse sections through the SE. By using standard light microscopy, each section was examined for the presence of [^{3}H]thymidine-labeled nuclei in the SE. The [^{3}H]thymidine-labeled cells were identified by the presence of five or more silver grains overlying the cell nucleus. Their numbers and locations were reported in Kuntz and Oesterle (1998).

Preparation of sections for transmission electron microscopy

Labeled cells in the SE were photographed, and the light photomicrographs were subsequently used to identify them at the TEM level. The thick (3 μm) sections were then re-embedded for TEM by using the method of King et al. (1982) and Presson et al. (1996). Beem capsules filled with unpolymerized epoxy resin Embed 812 (Electron Microscopy Sciences, Ft. Washington, PA) were inverted over the section and partly polymerized at 75°C. The capsule was then popped off the slide, with the section laying flat on the bottom surface of the partly polymerized block. After further polymerization, ultrathin (90 nm) sections were made and mounted on carbon-stabilized, Formvar-coated slotted grids. Sections were stained with uranyl acetate and lead citrate, and viewed on a JEOL 1200 EX transmission electron microscope. The labeled cells were identified with the aid of light photomicrographs taken previously. The location, size, and shape of neighboring structures allowed for reliable identification of the labeled cell.

With this method, a portion of a labeled cell (3 μm) can be serially sectioned for TEM. Unfortunately, technical limitations of the method prevent serial sectioning of the entire cell. Labeled cells are thicker than 3 μm and encompassed by two or more serial thick sections. Because of the positions of the sections on the slide, adjacent sections could not always be popped off. In addition, sections could only be popped off the same glass slide three times before remaining sections became too hardened to be removed (glass slides break before section can be removed).

RESULTS

Structure of the sensory epithelium

The rat vestibular SE contains supporting cells (SCs), nerve fibers, terminals, and sensory hair cells (HCs). Two types of HCs are present: Type I HCs are flask-shaped and enclosed in a nerve calyx, whereas type II HCs are cylindrical and have multiple bouton-type nerve endings. The nuclei of both HC types lie in the lumenal two thirds of the SE, and stereocilia rise from HC lumenal surfaces. Supporting cell nuclei are positioned close to the basal lamina, and the basal portions of the SCs abut the basement membrane. Supporting cells, in contrast to HCs, span the entire distance of the epithelium. Microvilli rise from SC lumenal surfaces, and SC cytoplasm is filled with numerous membrane-bound granules. The SCs possess a reticular membrane (Engström, 1961), a dark band below the apical surface (Fig. 1) thought to consist of densely packed actin filaments (Takumida et al., 1995). Pump implantation and infusion of tritiated-thymidine into the basal turn of the rat cochlea does not disrupt the normal cytoarchitecture of the utricular macula, and the macula does not demonstrate evidence of morphologic damage (Kuntz and Oesterle, 1998; Fig. 1).

Labeled sensory epithelial cells are absent in undamaged (control) animals

Tritiated-thymidine–labeled SE cells are virtually absent in the utricular maculae of the normal undamaged control animals, indicating an absence of ongoing cell proliferation (Table 1, Fig. 1). In a total of 12 animals (where all serially sectioned semi-thin (3-μm) sections of the utricular maculae were examined for each utricle), only one labeled nucleus was seen in the SE. Hence, labeled cells were not available for ultrastructural analysis at the TEM level.

Drug-induced lesion

To damage HCs, 0.1 mg of gentamicin sulfate was placed into the catheter, and the 3-day osmotic pump was filled with [^{3}H]thymidine or TGFα (5 μg) plus insulin (100 μg) in [^{3}H]thymidine. In previous work (Kuntz and Oesterle, 1998), we described and quantified the amount of gentamicin-induced damage to the utricular macula. HCs are damaged, as evidenced by nuclear pyknosis, cytoplas-

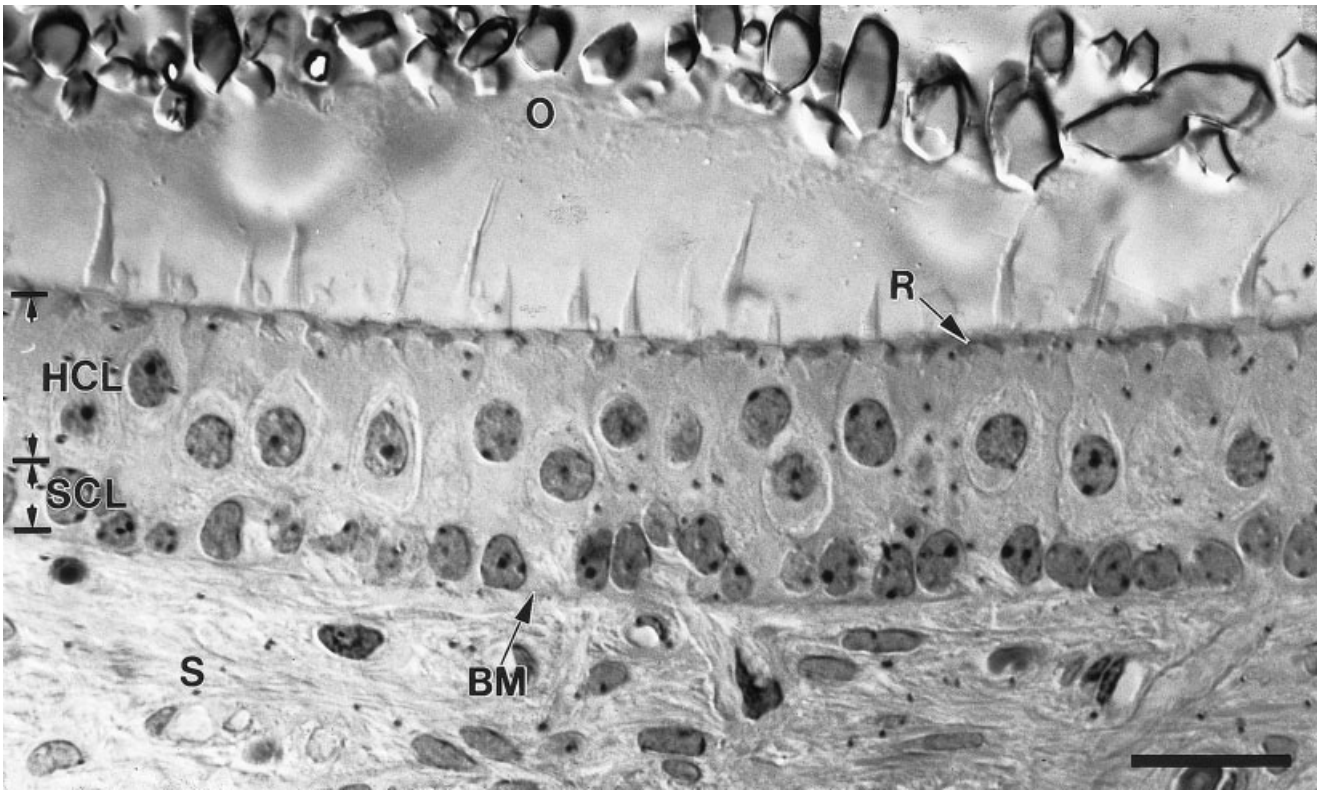

Fig. 1. Vestibular sensory epithelium (utricular macula) from a normal undamaged (control) adult rat. The rat was infused with [^{3}H]thymidine for 3 days and killed 1 day later, on day 4 after pump placement. Hair cells and supporting cells do not demonstrate evidence of damage from the osmotic pump implantation. Note the absence of [^{3}H]thymidine-labeled cells in the sensory epithelium. HCL, hair cell nuclear layer; SCL support cell nuclear layer; BM, basement membrane; O, otoconia; R, reticular membrane; S, stroma. Scale bar = 20 μm.

mic extrusion, vacuolization, and stereociliary fusion apparent in many HCs. Other signs of sensory epithelial damage include a marked disruption of nuclear layers. Nuclei are scattered throughout the SE instead of being arranged in their normal discrete layers. Numbers of pyknotic nuclei are significantly greater ($P < 0.01$) in drug-damaged tissue (mean = 7.1×10^{-5} pyknotic nuclei/μm^3, SE $\pm$ 1.4×10^{-5} SEM) than in normal control tissue (mean = 1.6×10^{-6} pyknotic nuclei/μm^3, SE $\pm$ 1.4×10^{-5} SEM).

Labeled sensory epithelial cells are present in experimental animals

Table 1 summarizes the mean number of [^{3}H]thymidine-labeled cells seen at the light microscope level in the utricular maculae of normal and gentamicin-damaged animals infused with either [^{3}H]thymidine or [^{3}H]thymidine with TGFα (5 μg) plus 100 μg insulin. The light microscope findings are reported in depth in Kuntz and Oesterle (1998). In the present study, 43 of these cells (taken from 10 animals) were examined with TEM to determine the ultrastructural properties of the labeled cells and to identify cell phenotype. Tritiated-thymidine–labeled cells located throughout the SE were analyzed; labeled cells located among HC nuclei in the lumenal two thirds of the SE were studied, as were labeled cells located in the basal third of the epithelium among SC nuclei. Because a major question was whether labeled HCs could be unequivocally found, we intentionally biased our sample of cells toward those with nuclei in the lumenal two thirds of the SE. In total, 20 of the 43 cells that were examined had their nuclei in the lumenal two thirds of the epithelium. We have identified five classes of [^{3}H]thymidine-labeled cells (presumptive HCs, SCs, leukocytes, nondescript or "active" cells, and degenerating HCs), and they are described below.

Labeled presumptive hair cells (synaptic specializations)

Labeled cells with synaptic specializations are rare; 2 were detected among the 43 labeled cells examined. Both of these cells were found in animals infused with gentamicin before a 3-day infusion with TGFα plus insulin and [^{3}H]thymidine. The labeled cells with synaptic specializations were located in the lumenal half of the SE. Figures 2 and 3 show a labeled cell with several primordial synaptic contacts with neural processes. Light photomicrographs of the labeled cell are shown in Figure 2a,b; a low magnification TEM of the labeled cell profile is shown in Figure 2c. Higher magnification TEMs illustrating three regions of the labeled cell with synaptic specializations with nerve fibers are shown in Figure 3. The lumenal surface of the cell was not present in the sections. Each synaptic region contains one or a few, but not all, of the features of a true

TABLE 1. Effect of TGFα Plus Insulin on Cell Proliferation in Rat Utricular Maculae on Normal and Gentamicin-Damaged Animals[1]

Paradigm	Addition(s)	n	Number labeled cells per utricular macula (mean ± SEM)
Normal 3d infusion	[^{3}H]thymidine	8	
	SC		0.0 ± 0.0
	HC		0.0 ± 0.0
	Total		0.0 ± 0.0
	[^{3}H]thymidine + 5 μg TGFα + 100 μg Insulin	9	
	SC		4.0 ± 0.8**
	HC		0.2 ± 0.1
	Total		4.2 ± 0.8**
Gentamicin-damaged 3d infusion	[^{3}H]thymidine	5	
	SC		16.9 ± 7.9*
	HC		5.3 ± 2.8*
	Total		22.3 ± 9.3*
	[^{3}H]thymidine + 5 μg TGFα + 100 μg insulin	5	
	SC		30.4 ± 12.8*
	HC		7.0 ± 5.5
	Total		37.2 ± 18.0*
Normal 7d infusion	[^{3}H]thymidine	4	
	SC		0.1 ± 0.1
	HC		0.0 ± 0.0
	Total		0.1 ± 0.1
	[^{3}H]thymidine + 5 μg TGFα + + 100 μg Insulin	7	
	SC		14.1 ± 3.7*
	HC		2.8 ± 0.9
	Total		17.2 ± 4.1*

*$P \leq 0.05$ vs. control.
**$P \leq 0.01$ vs. control.
[1]SC, supporting cell layer; HC, hair cell layer; 3d infusion, test agent(s) infused for 3 days and animal was killed 1 day later, 4 days after pump implantation; 7d infusion, test agent(s) infused for 7 days and animal was killed 3 days later, 10 days after pump implantation.

mature synapse. Hence, they are classified as primitive or primordial synapses (Newman-Gage and Westrum, 1984; Kunkel et al., 1987; Vaughn, 1989; Sobkowicz, 1992). The synaptic region indicated by the open arrow in Figure 3a is shown at a higher magnification in Figure 3b. A coated "pit" (62 nm in diameter; Fig. 3b, arrowhead) is fused with the presynaptic membrane or opening into the synaptic cleft. Several granulated (dense-cored) vesicles are nearby, and a variety of differently sized irregularly shaped vesicles and smooth endoplasmic reticulum are present. There are no obvious pre- or postsynaptic membrane specializations or thickenings, although the membrane segment on the soma appears dense. There also appears to be a "synaptic cleft" with parallel apposing membranes and amorphous synaptic cleft material. A different synaptic region on the same labeled cell is indicated by the arrowhead in Figure 3a, and a higher magnification of this region is shown in Figure 3c. A neural terminal (probably an efferent terminal) contains numerous synaptic vesicles and a collection of larger vacuolar structures suggestive of a growing neural process. This profile appears to form a contact with the labeled cell at a membrane specialization (arrowhead) with an obvious synaptic cleft adjacent to synaptic vesicles (sv). A third synaptic region on the labeled cell is indicated by the arrow in Figure 3a, and it is shown at a higher magnification in Figure 3d. A thin neural process with vacuoles (v) and a coated vesicle (cv) is directly apposed to the labeled cell with a dense membrane specialization (arrowhead). A nearby profile is contacted at a synaptic specialization (arrow) by a thin process containing vacuoles, coated vesicles, and a presynaptic density (d).

Gap junctions and other ultrastructural features characteristic of SCs (e.g., numerous membrane-bound granules) were not observed in these labeled cells which re-

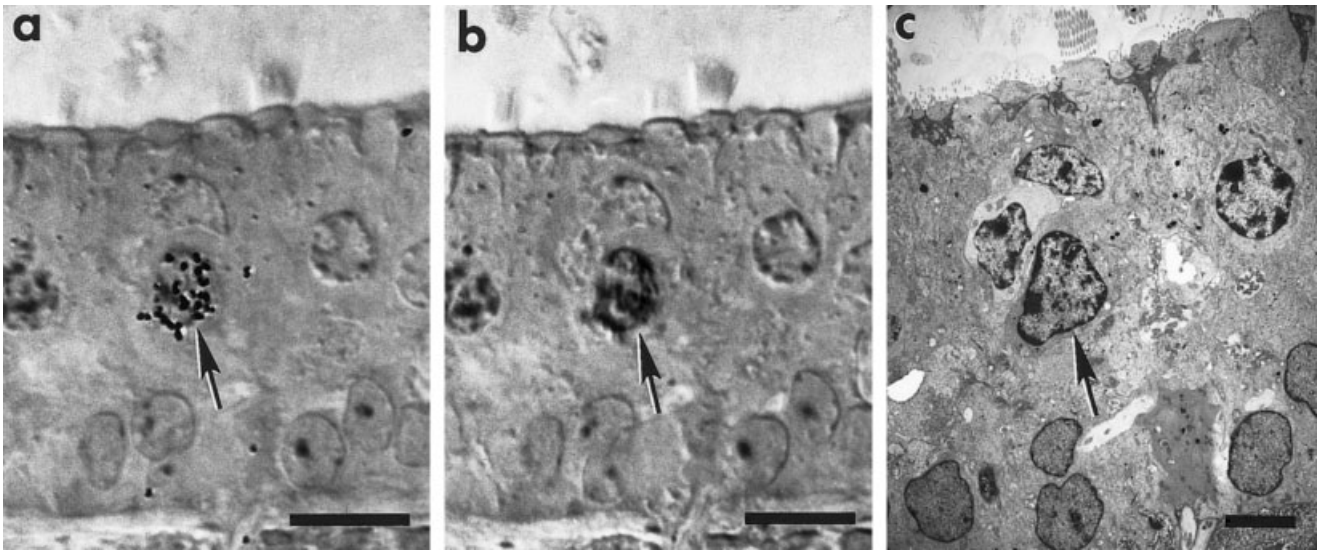

Fig. 2. Labeled cell with immature, primordial synaptic specializations with nerve fibers. **a:** Light photomicrograph taken from a gentamicin-damaged rat ear that was infused with [^{3}H]thymidine and 5 μg TGFα plus 100 μg insulin for 3 days and fixed 4 days after pump implantation. A labeled cell (arrow), a putative developing hair cell, is located in the lumenal half of the sensory epithelium. The focus is on the silver grains. **b:** Light photomicrograph of the labeled cell (arrow) with the focus on the cell nucleus. **c:** Low magnification electron micrograph of the labeled cell (arrow) profile. Hair cell nuclei and the nuclei of the labeled cell display heterochromatin (clumping of dense nuclear chromatin at the periphery), whereas the supporting cell nuclei are euchromatic (i.e., homogenously granular with prominent nucleoli). Scale bars =10 μm in a,b, 5 μm in c.

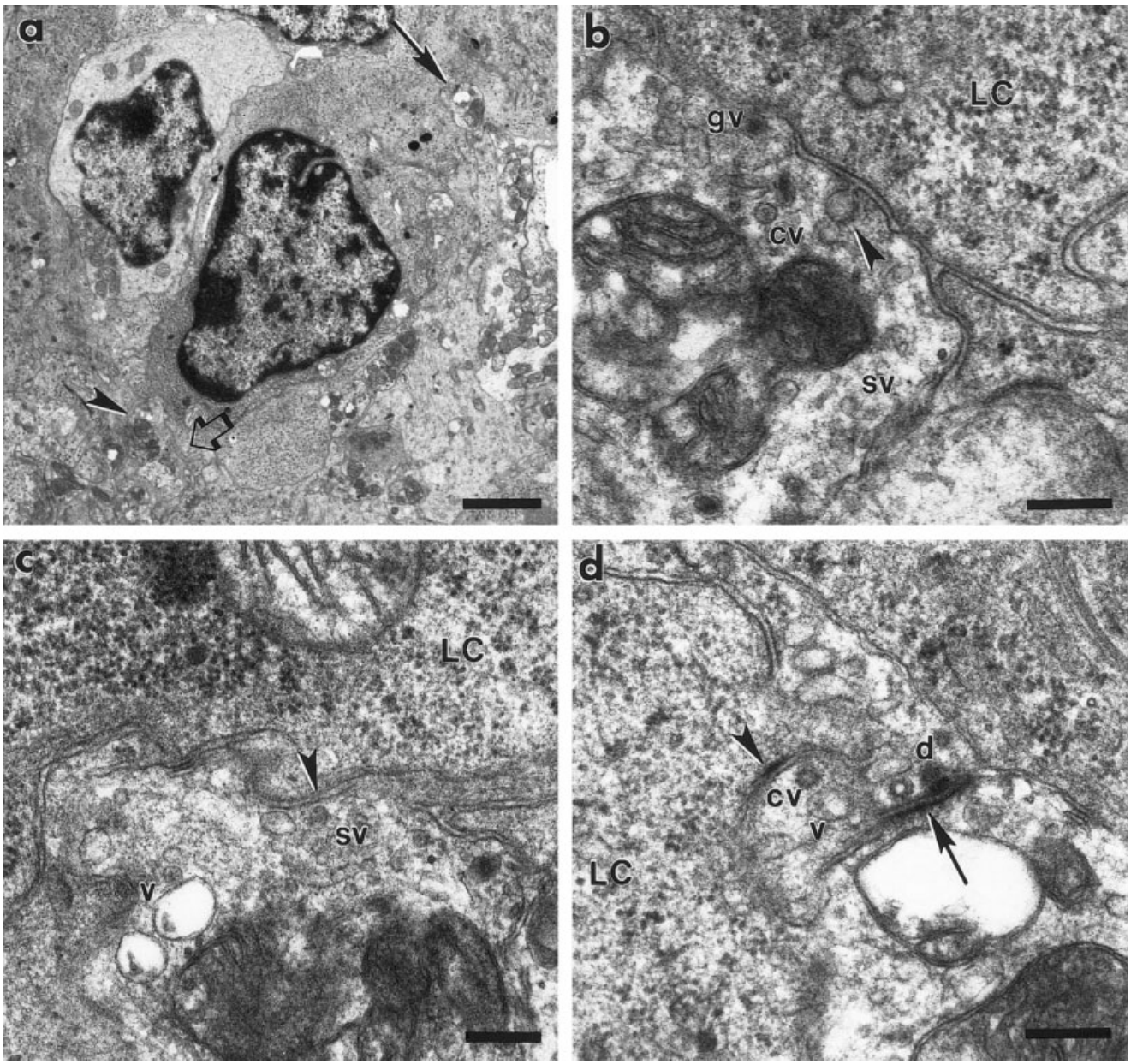

Fig. 3. Higher magnification of the primordial synaptic specializations on the labeled cell shown in Figure 2. **a:** Numerous neural elements abut the labeled cell. Regions with primordial neural synapses are indicated by the open arrow, arrowhead, and arrow, and they are shown at higher magnifications in parts b, c, and d, respectively. **b:** Higher magnification of the region indicated by the open arrow in part a in an adjacent thin section. A coated vesicle (cv, arrowhead) fused with the membrane of a presumed efferent fiber juxtaposed to the labeled cell (LC). Several granulated (dense-cored) vesicles (gv) and possible synaptic vesicles (sv) of various shapes are present in the presynaptic element. The fused vesicle is opening into a possible synaptic cleft at which the opposing membranes have parallel appositions with a suggestive increased density. **c:** Higher magnification of the region in part a indicated by the arrowhead. Synaptic vesicles (sv, 40–46 nm in diameter) as well as smooth reticulum are clustered in several sites in the neural process, a presumed efferent fiber, contacting (arrowhead) the labeled cell (LC). v, vesicles or vacuoles. **d:** Higher magnification of the region in part a indicated by the arrow. A membrane specialization (arrowhead) is present on the labeled cell (LC) abutting a presumed nerve fiber. A coated vesicle (cv) can be seen near the contact. A second asymmetric membrane specialization (arrow) is also apparent in a neural element in contact with a second neighboring neural element. d, presynaptic dense projection; v, vacuole. Scale bars = 2 μm in a, 200 nm in b–d.

ceive neural contacts with primordial specializations. This, combined with the general dogma that SCs in mammalian vestibular epithelia do not receive innervation, lead us to speculate that this cell is a newly generated HC with developing synaptic specializations (with efferent and possibly afferent fibers).

The second labeled cell detected with synaptic specializations has more mature specializations; it has clearly

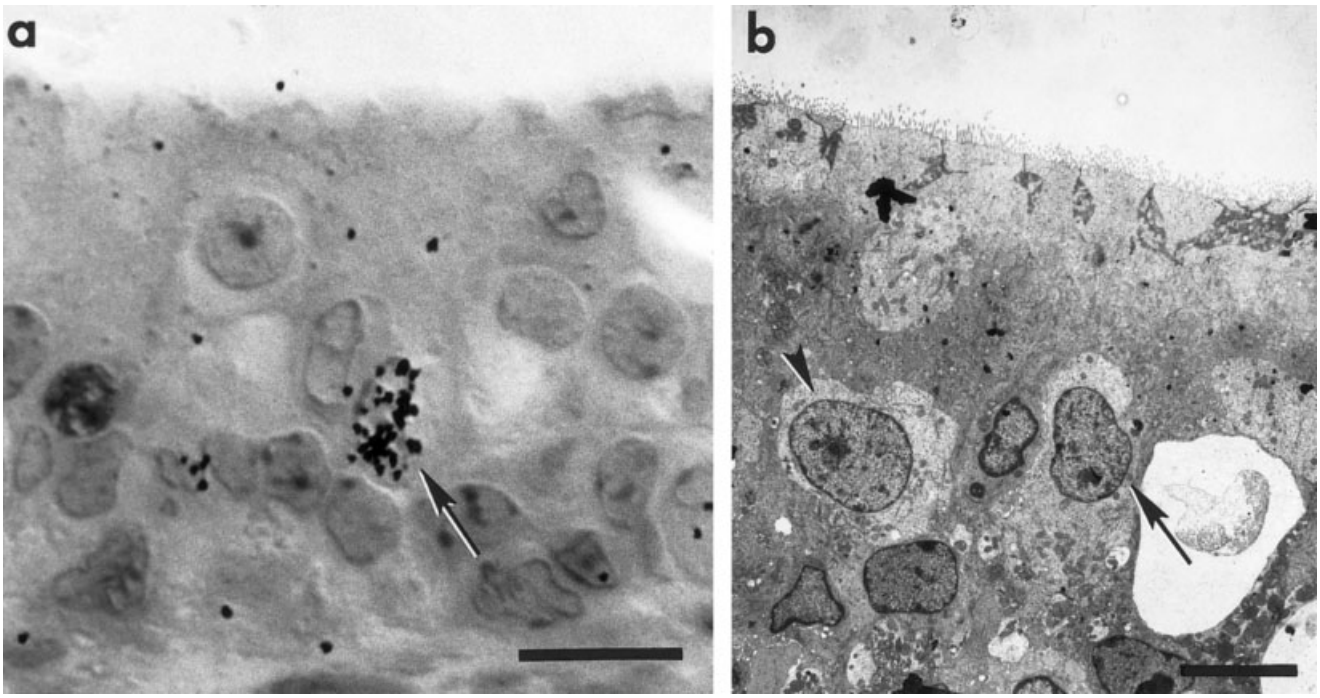

Fig. 4. Labeled cell showing synaptic specializations with afferent and efferent terminals. **a:** Light photomicrograph taken from a gentamicin-damaged rat ear that was infused with [^{3}H]thymidine and 5 μg TGFα plus 100 μg insulin for 3 days and fixed 4 days after pump implantation. A clearly labeled cell (arrow) is located in the lumenal half of the sensory epithelium. The focus is on the silver grains. **b:** Section shown in part a processed for transmission electron microscopy. The arrow points to the labeled cell of part a, a labeled hair cell. The cytoplasm of the labeled cell is electron lucent like that of nearby unlabeled hair cells (arrowhead) and lighter than that of adjacent unlabeled supporting cells. Scale bars = 10 μm in a, 5 μm in b.

identifiable presynaptic bodies opposed to afferent terminals. A light photomicrograph of this cell is shown in Figure 4a, and higher magnification electron micrographs of three synaptic regions are shown in Figure 5. The lumenal region of the labeled cell is not present in the sections. In the cell's basal region, presynaptic vesicles encircle a synaptic body (Fig. 5c, black arrow). A distinct postsynaptic specialization (Fig. 5c, open arrow) is obvious in the presumed afferent terminal (AN). Efferent terminals make contact with the labeled cell as shown in Figure 5c. A postsynaptic cistern of smooth endoplasmic reticulum can be seen in the labeled cell at the apposition of the efferent terminal (arrowhead). The cytoplasm of the labeled cell is electron lucent like that of nearby unlabeled HCs and lighter than that of adjacent unlabeled SCs (Figs. 4b, 5a). Similar to the other labeled HC, gap junctions were not observed, and numerous membrane-bound granules, a characteristic feature of SCs, were not detected in the cytoplasm. Hence, this cell is thought to be a labeled HC in synaptic contact with afferent and efferent terminals.

Ultrastructural characteristics of the labeled HC were carefully examined to assess whether the cell appeared to be dying or damaged. Ultrastructural features characteristic of dying cells are not seen in this cell. Minimal mitochondrial swelling is present, and lysosomes are extremely rare. The cell is not swollen, and the nucleus has a normal appearance without the presence of nuclear membrane breakdown or marked nuclear chromatin "clumping." The rough endoplasmic reticulum and ribosomes are intact, and there is no detectable evidence of ribosomal lysis. The absence of characteristic features of degenerating cells suggests that this labeled cell is newly generated, not a damaged HC that has re-entered the cell cycle.

Labeled supporting cells

Eleven labeled cells could be classified as sensory epithelial supporting cells on the basis of their ultrastructural characteristics. The labeled SCs were found in animals infused with TGFα plus insulin and [^{3}H]thymidine for 7 days and fixed on day 10. Of interest, the majority (73%) of the labeled SCs had nuclei located in the middle (n = 5) or upper (lumenal) half of the SE (n = 3). Three of the 11 labeled SCs (27%) had nuclei located in the lower (basal) half of the SE, the region where SC nuclei are typically located. An example of a labeled SC is shown in Figure 6. The nucleus of this labeled cell is located in the lower half of the SE (Fig. 6a,b). The nucleus is rectangular and has a prominent nucleolus in addition to aggregates of nuclear chromatin ("heterochromatic") suggestive of an inactive/resting nucleus. The labeled SC in Figure 6 looks different than the surrounding unlabeled SCs, as its cytoplasm is more electron dense. A higher magnification of the labeled cell is shown in Figure 6c, and the asterisks indicate some of the numerous membrane-bound granules ringed by ribosomes characteristically found in the SC cytoplasm. These granules are moderately electron-dense with fine granular elements. Numerous microvilli rise from the apical surface of the labeled SCs (Fig. 6b), and a

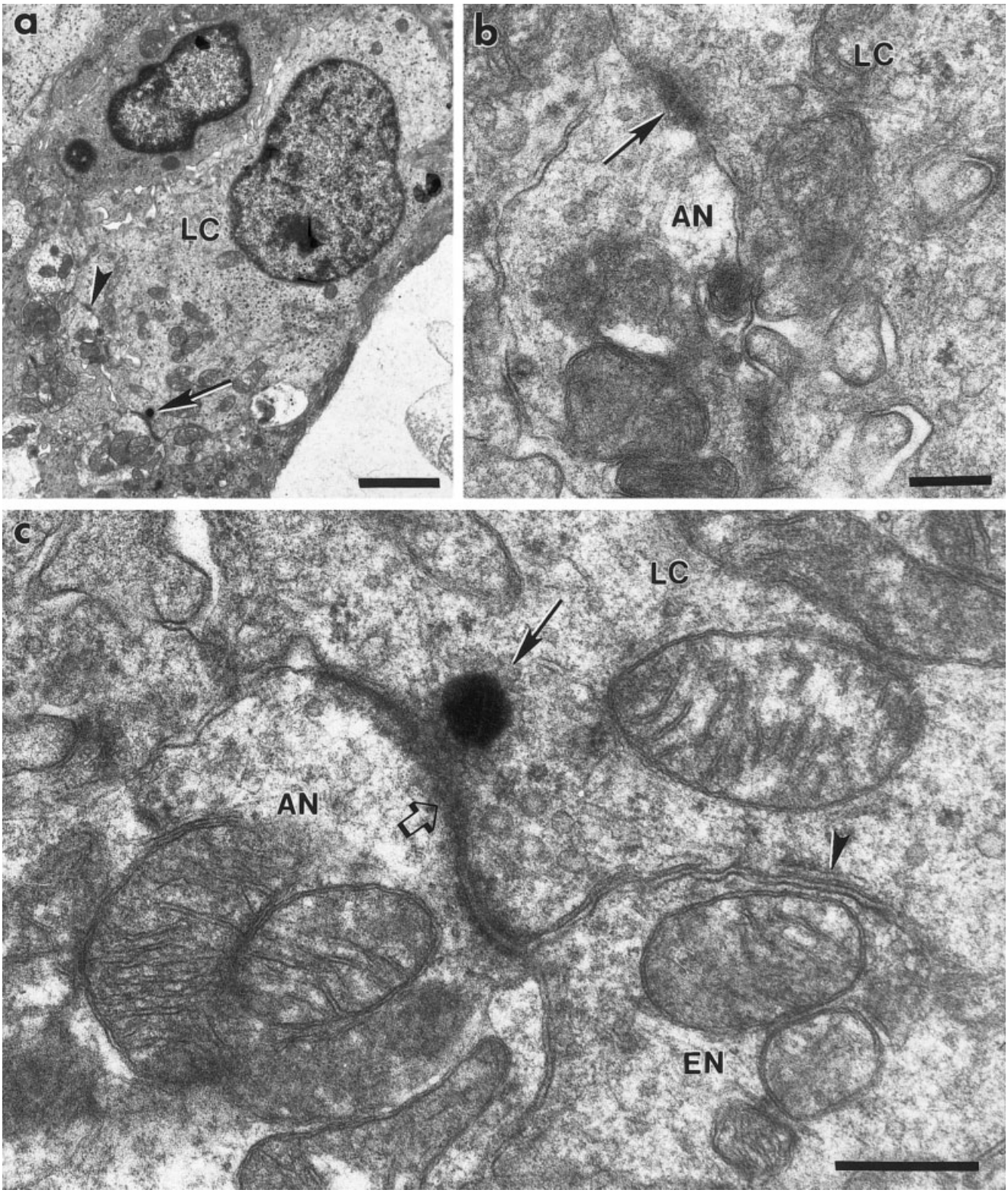

Fig. 5. Higher magnification of synaptic specializations on the labeled cell shown in Figure 4. **a:** Numerous neural elements abut the labeled cell (LC). The arrowhead and arrow point to regions of the labeled cell with synaptic specializations. **b:** Higher magnification of the region indicated by the arrowhead in part a. A membrane density (arrow) can be seen on a presumed afferent neural element (AN) at a contact with the labeled cell (LC). **c:** Higher magnification of the region indicated by the arrow in part a. Note the round synaptic body (black arrow) in the labeled cell (LC) opposite an afferent nerve (AN) terminal and the membrane thickenings (open arrow) of the synaptic membranes. A presumed efferent terminal (EN) also apposes the labeled cell, adjacent to subsurface cisternae (arrowhead) in the labeled cell. Scale bars = 2 μm in a, 250 nm in b, 200 nm in c.

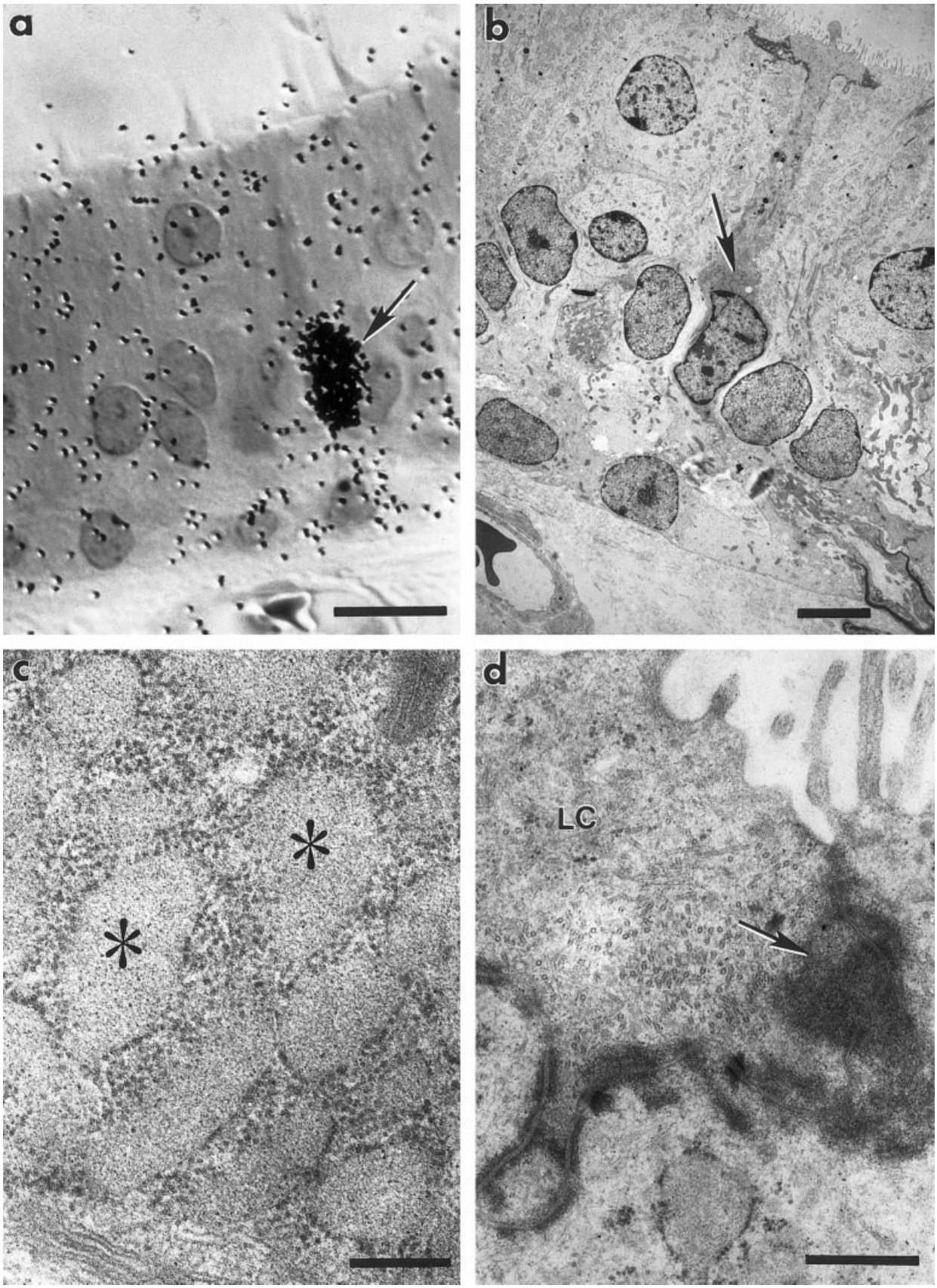

Fig. 6. A labeled supporting cell in the rat vestibular sensory epithelium (SE). Section from a normal rat utricle continuously infused with transforming growth factor alpha plus insulin and [^{3}H]thymidine for 7 days and fixed 10 days after pump implantation. **a:** Light photomicrograph of a thick section with a [^{3}H]thymidine-labeled nucleus (arrow) in the SE. **b:** Section shown in part a processed for transmission electron microscopy. The arrow points to the labeled cell in part a, a labeled supporting cell. Note the lumenal microvilli. **c:** Higher magnification of the region indicated by the arrow in part b, showing some of the numerous membrane-bound granules ringed by ribosomes (e.g., asterisks) in the labeled supporting cell. **d:** Higher magnification of the apical region of the labeled cell (LC). Note the dark staining granular substance (arrow). Scale bars = 10 μm in a, 5 μm in b, 250 nm in c, 500 nm in d.

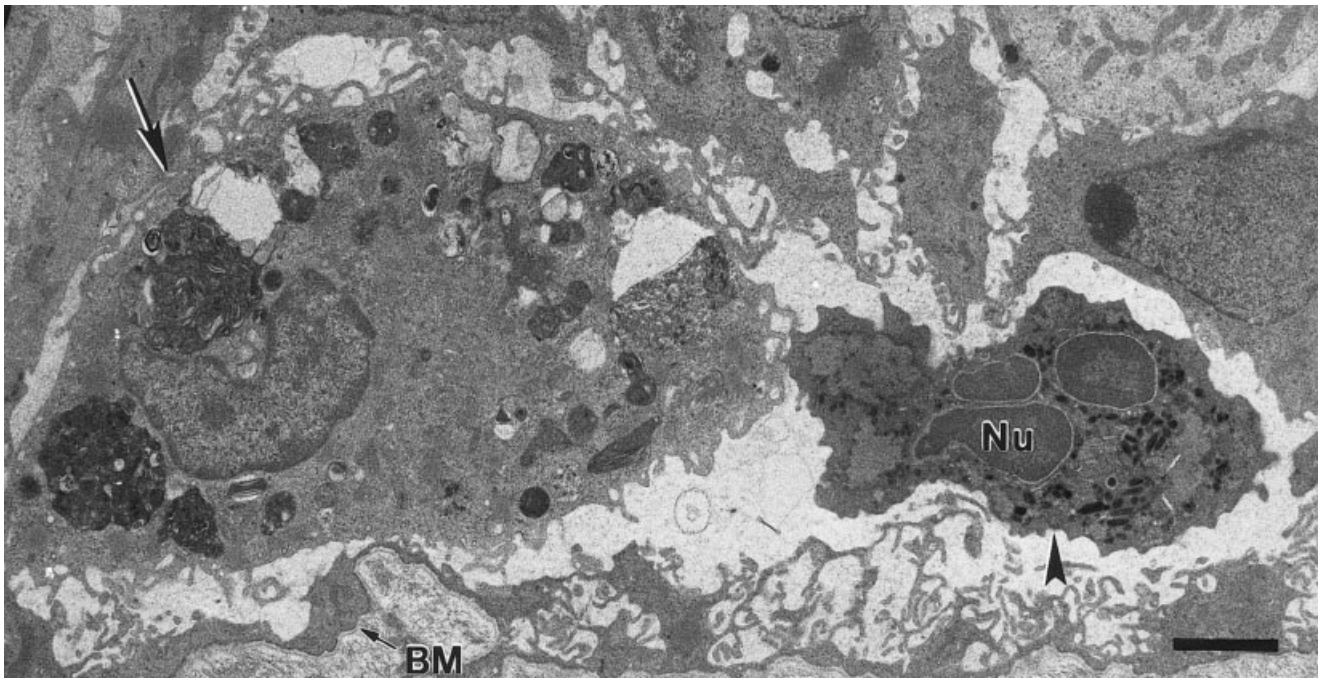

Fig. 7. Labeled leukocytes in the rat vestibular epithelium. An ultrathin section from a normal rat utricle that was continuously infused with [^{3}H]thymidine and transforming growth factor alpha plus insulin for 7 days and fixed 10 days after pump implantation. A macrophage (arrow) with extensive inclusions and a neutrophil (arrowhead) with a lobulated nucleus (Nu) are located in the sensory epithelium near the basement membrane (BM). The macrophage was labeled with [^{3}H]thymidine (not shown). Scale bar = 2 μm.

dark staining, granular substance often forms a filament band near the apex of the cell (Fig. 6d, arrow). Longitudinal bundles of microtubules (2–15) were sometimes seen in the labeled SCs (not shown). Labeled SCs often interdigitated extensively with unlabeled SC neighbors.

Labeled leukocytes

Both unlabeled and [^{3}H]thymidine-labeled leukocytes (n = 6) were seen in the utricular maculae of the pump-implanted rats. Five of the six labeled leukocytes were observed in gentamicin-damaged animals, and one was seen in an undamaged, growth factor–supplemented animal. Based on ultrastructural characteristics, a variety of leukocyte subtypes were observed, including lymphocytes, macrophages, and neutrophils. A [^{3}H]thymidine-labeled macrophage is shown in Figure 7 (arrow). The macrophage is 14 μms in diameter with an irregularly shaped nucleus and numerous finger-like processes extending from the surface of the cell, indicating a high surface activity. Dense bodies of varying size and internal structure are conspicuous components of the cytoplasm. Some of these bodies appear to be primary lysosomes, phagosomes, and secondary lysosomes (phagolysosomes) with diverse internal structure where phagocytosed particles are digested.

An unlabeled neutrophil (8 μms in diameter) abuts the labeled macrophage. In this ultrathin section, the three lobes of the lobulated nucleus of the neutrophil appear as individual segments. The chromatin has a dense structure, and large clumps of the condensed chromatin adhere to the nuclear membrane. Numerous granules, ovoid or elongated in shape, are present in the cytoplasm that otherwise contains few cell organelles. A moderately electron-opaque, amorphous background material is present. An example of a [^{3}H]thymidine-labeled lymphocyte (7 μms in diameter) is shown in Figure 8. Light photomicrographs and a low-magnification electron micrograph of the labeled cell are shown in Figure 8a,b, and c, respectively. A higher magnification electron micrograph of the labeled lymphocyte is shown in Figure 8e. The nucleus of the labeled cell is oval and contains a prominent nucleolus. A narrow rim of cytoplasm surrounds the nucleus with numerous ribosomes in the cytoplasm.

Labeled nondescript cells

Approximately half (51%, n = 22) of the labeled cells examined were relatively nondescript cells, except that they contain massive numbers of ribosomes. They did not contain ultrastructural features characteristic of HCs or mature SCs. We have termed these cells "active cells," on the basis of the massive numbers of polyribosomes that suggest that they are metabolically active. However, their nuclei are heterochromatic, suggesting nonactive states. Tritiated-thymidine–labeled active cells were seen in normal animals infused with TGFα plus insulin, drug-damaged animals not infused with growth factor, and drug-damaged animals infused with TGFα plus insulin. The active cells range between 5 and 15 μms in diameter (average diameter = 9 μms ± 3 μms SD) and tend to be located near the basement membrane (91%, n = 20; e.g., Fig. 9; one contacted the basement membrane directly), but two were detected in the lumenal portion of the epithelium (e.g., Fig. 8a–d). Active cells typically have a cytoplasmic density similar to that of neighboring SCs

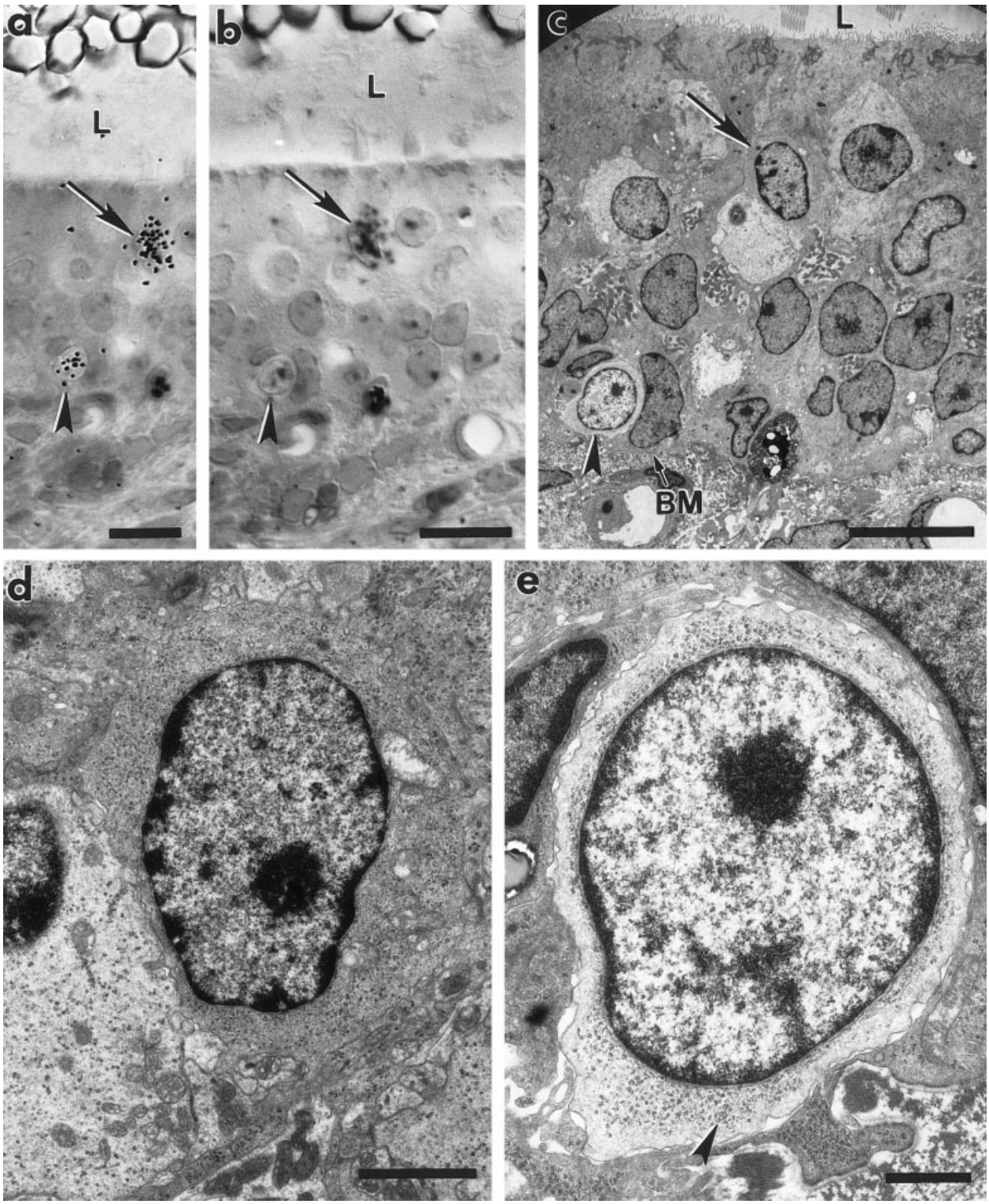

Fig. 8. A [^{3}H]thymidine-labeled lymphocyte and a labeled nondescript cell we have termed an "active cell." **a,b:** Light photomicrographs from a gentamicin-damaged rat utricle that was continuously infused with [^{3}H]thymidine and transforming growth factor alpha plus insulin for 3 days and fixed 4 days after pump implantation. Note the presence of a labeled lymphocyte (arrowheads) located near the basement membrane and a labeled active cell in the lumenal half of the sensory epithelium (arrows). The plane of focus in parts a,b is on the silver grains and on the nuclei, respectively. L, lumen. **c:** Section shown in parts a,b processed for transmission electron microscopy. The arrow points to the lumenally located labeled cell of parts a,b, and the arrowhead points to the basally located labeled cell. BM, basement membrane. **d:** Higher magnification of the labeled active cell in a thin section adjacent to that shown in part c. Active cells are nondescript, except that they contain massive numbers of polyribosomes. Note the numerous polyribosomes. **e:** Higher magnification of the labeled lymphocyte in a thin section adjacent to that shown in part c. Note the electron lucent cytoplasm of the cell, the numerous polyribosomes (e.g., arrowhead), and the scarcity of other organelles. Scale bars = 20 μm in a,b, 10 μm in c, 2 μm in d, 1 μm in e.

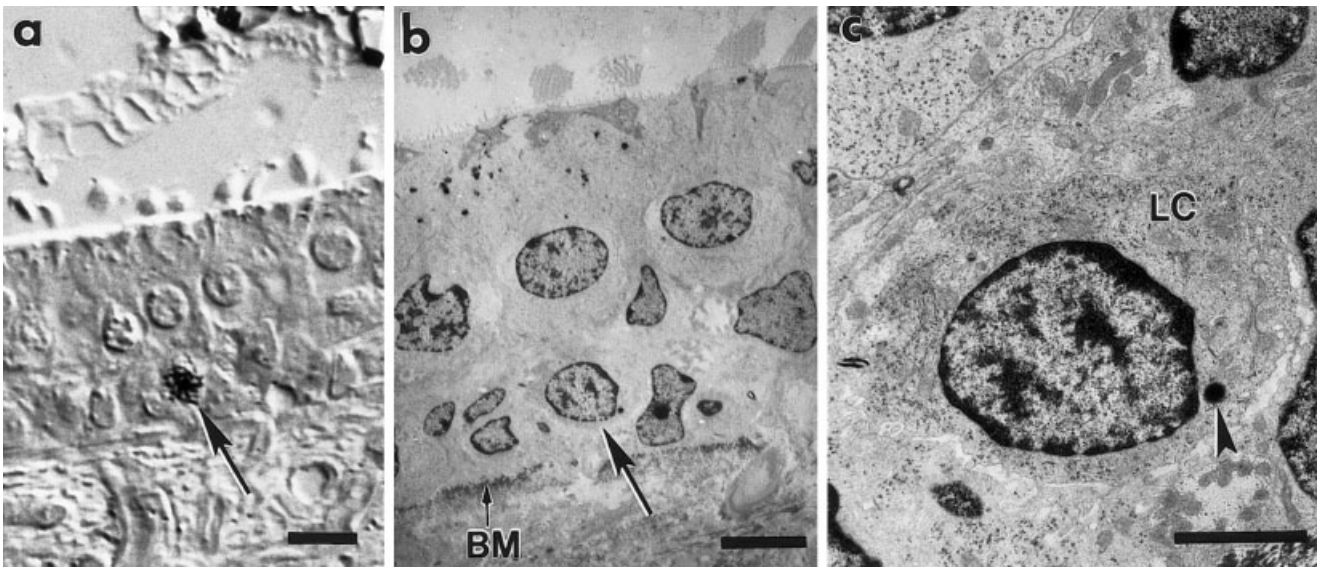

Fig. 9. An "active cell" labeled with [^{3}H]thymidine located near the basement membrane. **a:** Light photomicrograph from a gentamicin-damaged rat utricle that was continuously infused with [^{3}H]thymidine for 3 days and fixed 4 days after pump implantation. Note the [^{3}H]thymidine-labeled nucleus (arrow) located near the basement membrane. **b:** Section shown in part a processed for transmission electron microscopy. Arrow points to the labeled cell in part a, a labeled active cell. BM, basement membrane. **c:** Higher magnification of the labeled active cell (LC) in parts a,b. Note the numerous polyribosomes. Active cells also have numerous small filopodia (not shown) and occasional dense inclusions (arrowhead). Scale bars = 10 μm in a, 5 μm in b, 2 μm in c.

(Figs. 8c,d, 9). Active cells have numerous small filopodia and occasional dense inclusions (e.g., Fig. 9c arrowhead). Microtubule fascicles have been observed in some active cells. Membrane contacts between active cells and adjacent unlabeled cells consist of increases in membrane density with parallel alignment of the membranes, and an occasional desmosomal-like contact has been seen. Gap junctions have not been observed between active cells and neighboring cells. Neural contacts with active cells have not been observed, even though neural processes can be in close proximity.

Labeled degenerating cells

Two degenerating cells labeled with [^{3}H]thymidine were detected in the gentamicin-damaged ears (Figs. 10, 11). These cells were located in the lumenal portion of the epithelium among the HCs. One of the labeled cells appeared to be a degenerating HC (Fig. 10) because of the apparent neural contacts and lumenal location of the nucleus. The nucleus of the labeled HC is irregular, multilobed, and relatively electron lucent. Condensed chromatin is apparent around the nuclear periphery. Primary and secondary lysosomes are present in the cytoplasm (Fig. 10d) Polyribosomes can be seen in the cytoplasm, and ribosomes are present on the rough endoplasmic reticulum. Several neural elements are juxtaposed to the labeled cell; two of these are shown at a higher magnification in Figure 10c.

A [^{3}H]thymidine-labeled cell that has progressed farther along the degenerative pathway is shown in Figure 11. The dying cell contains a small amount of dark cytoplasm, and the nucleus is electron dense. The nucleus to cytoplasm ratio of the cell is high. The darkness of the cytoplasm makes the details of the intracellular structure indiscernible. Consequently, cell type cannot be determined. However, the lumenal location of the dying cell suggests it is a dying HC.

DISCUSSION

The findings reported here suggest that (1) new vestibular hair cells may be produced by means of a mitotic pathway in the in situ adult rat inner ear, (2) gentamicin and/or TGFα plus insulin infusion stimulates the production of new sensory epithelial cells, (3) a variety of leukocyte subtypes can be present within adult rat vestibular epithelium and, (4) some leukocytes within the epithelium may proliferate. Data are also consistent with the idea that, upon damage, hair cells may attempt to re-enter the cell cycle, and this then triggers entrance into a cell death pathway and hair cell death.

Production of new hair cells in mature mammalian vestibular SE

Regenerated HCs in the avian auditory SE, the basilar papilla (homologue to the mammalian organ of Corti), are known to receive new afferent and efferent neural contacts with all of the normal synaptic specializations (Duckert and Rubel, 1990, 1993; Ryals et al., 1992; Ryals and Westbrook, 1994; Westrum et al., 1999). After gentamicin insult to the basilar papilla, nerve fibers remain in the position they occupied before the gentamicin damage, but the terminals either die back (afferents) or linger near the lumen (efferents). Efferent fibers and their terminals remain within the SE in areas of HC loss, although their morphologic appearance is greatly altered (Ofsie et al., 1997). Reinnervation of the regenerating HCs is thought to require the "sprouting" of new nerve terminals from the existing fibers to form connections with the differentiating

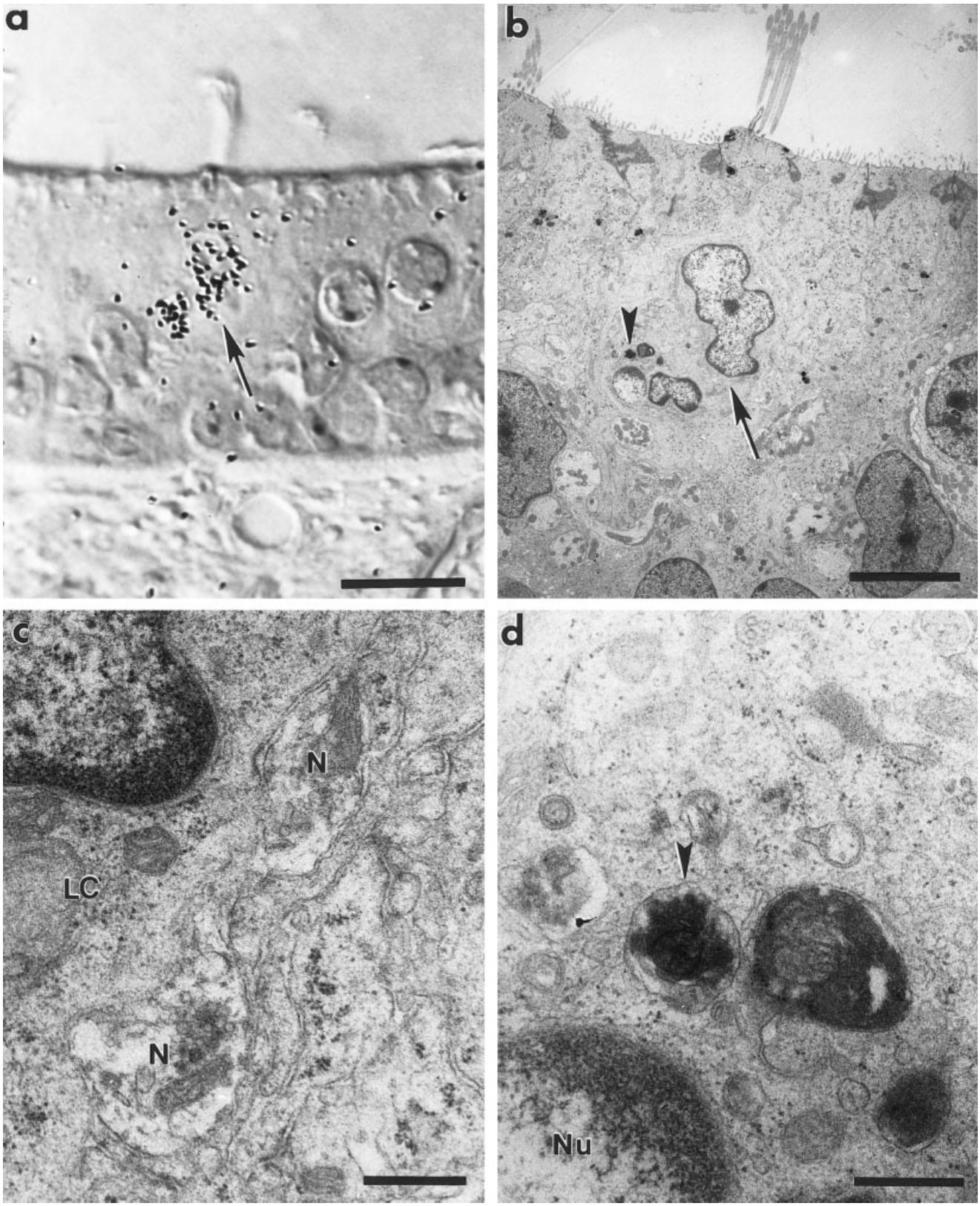

Fig. 10. A degenerating hair cell labeled with [^{3}H]thymidine. **a:** Light photomicrograph from a gentamicin-damaged ear that was infused with [^{3}H]thymidine for 3 days and fixed on day 4. **b:** Section shown in part a processed for transmission electron microscopy. The arrow points to the labeled cell shown in part a, a labeled hair cell that is degenerating. The arrowhead points to a region with lysosomes. **c:** Higher magnification of the labeled cell (LC) showing two juxtaposed neural elements (N). The lower neural element has synaptic vesicles. **d:** Higher magnification of the region with lysosomes indicated by the arrowhead in part b. The arrowhead points to one of several lysosomes present in the labeled cell. Nu, nucleus. Scale bars = 20 μm in a, 5 μm in b, 500 nm in c,d.

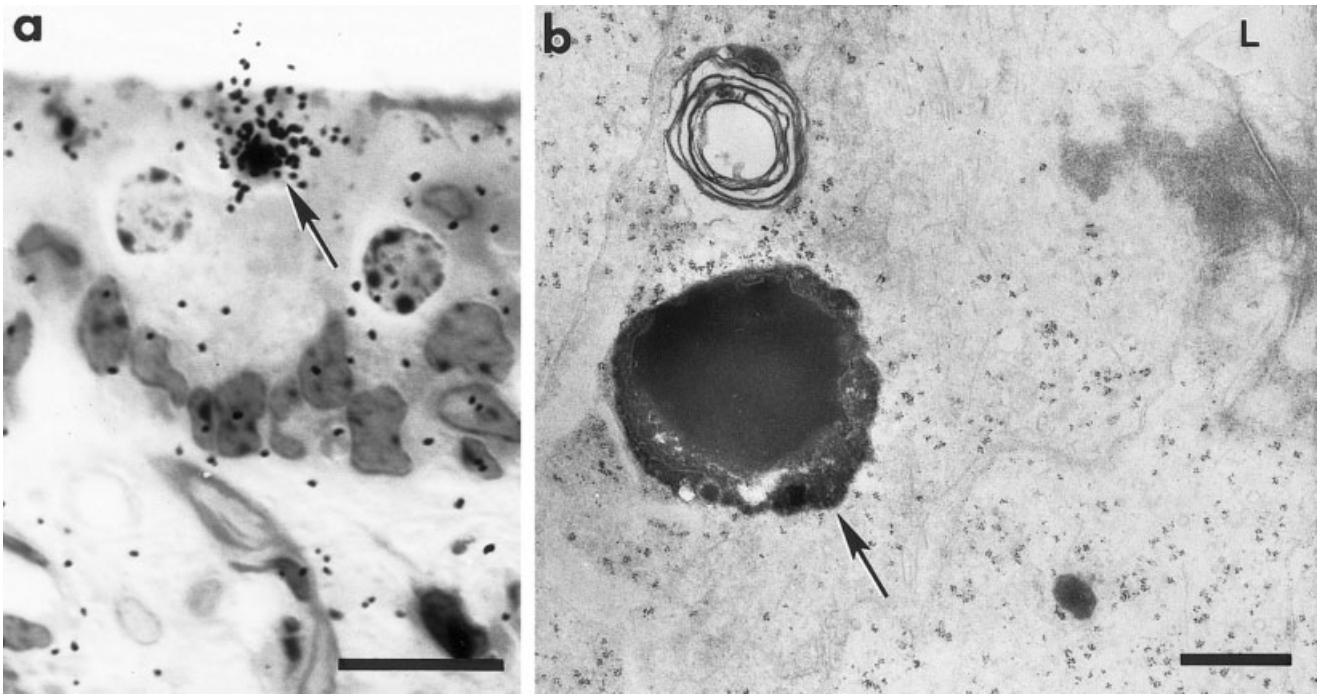

Fig. 11. A dying cell labeled with [^{3}H]thymidine. **a:** Light photomicrograph from a gentamicin-damaged ear that was infused with [^{3}H]thymidine for 3 days and fixed on day 4. Note the labeled cell (arrow) in the lumenal portion of the sensory epithelium. **b:** Section shown in part a processed for transmission electron microscopy. The arrow points to the labeled cell shown in part a, a labeled dying cell. L, lumen. Scale bars = 10 μm in a, 1 μm in part b.

sensory cells (Ofsie et al., 1997). Analogous studies remain to be conducted in regenerating avian vestibular sensory epithelia. Hence, little is known regarding the details of the reinnervation process of drug-damaged vestibular sensory epithelia.

Descriptions of the fine structure of afferent and efferent synapses on vestibular HCs in developing and adult rodents have been provided by several investigators (e.g., Wersäll. 1956; Engström et al., 1974; Nordemar, 1983; Sánchez-Fernández and Rivera-Pomar, 1983; Favre et al., 1986; Park et al., 1987; Mbiene et al., 1988; Lysakowski, 1996; Lysakowski and Goldberg, 1997; Ross, 1997; Rüsch et al., 1998; Kirkegaard and Jørgensen, 2001). Synaptogenesis in the vestibular SE has also been studied in other species, including cats (Favre and Sans, 1977, 1979; Favre et al., 1986), chickens (Ginzberg and Gilula, 1980), and humans (Sánchez-Fernández and Rivera-Pomar, 1983; Sans and Dechesne, 1987). Among the characteristic features at vestibular HC-neural synapses are the existence of specialized presynaptic bodies or ribbons in the HC at afferent synapses (Hamilton, 1968; Engström et al., 1974; Favre and Sans, 1979; Lysakowski, 1996), a subsynaptic cistern along the postsynaptic membrane of the HC at the efferent synapses (Ginzberg and Gilula, 1980), and efferent terminals packed with 40- to 60-nm clear synaptic vesicles (Favre and Sans, 1977; Ginzberg and Gilula, 1980). Afferent terminals can exhibit a postsynaptic density opposite the presynaptic body (Ginzberg and Gilula, 1980; Favre et al., 1986) and may have an assortment of vesicular structures but lack proper synaptic vesicles.

Primordial synaptic contacts can possess one or a few, but not all, of the features of a true mature synapse (Newman-Gage and Westrum, 1984; Kunkel et al., 1987; Vaughn, 1989). We observed a labeled cell with primordial synapses in a drug-damaged animal infused with TGFα plus insulin. Several primordial synaptic contacts were observed on this cell, a cell that is located in the lumenal region of the macula. We considered the cell to be a developing HC because of the presence of the synaptic contacts and the absence of ultrastructural features characteristic of supporting cells (e.g., large numbers of membrane-bound granules, gap junctions). One primordial synaptic profile contained an asymmetrical dense membrane specialization (Fig. 3d). During synaptogenesis, membrane densities frequently line presumptive pre- or postsynaptic elements in the developing central nervous system (Westrum et al., 1983; Newman-Gage and Westrum, 1984; Kunkel et al., 1987; reviewed in Vaughn, 1989), and asymmetrical membrane densifications were reported in developing vestibular HCs in mouse (Mbiene et al., 1988). Two of the primordial synaptic profiles contained coated vesicles (Fig. 3b,d). One coated vesicle, a coated pit, was in fusion with the presynaptic membrane. Coated "omega-like" pits are commonly found near developing synaptic contacts and have been suggested to be involved in adding molecules to presynaptic, as well as postsynaptic membranes (reviewed in Vaughn, 1989). Coated vesicles are also thought to play a role in the formation of synaptic vesicles within developing, as well as mature, presynaptic elements.

To date, SCs have not been reported to receive innervation in developing or mature mammalian vestibular epithelia. Hence, we tentatively considered labeled cells with synaptic specializations to be regenerating HCs. However,

we cannot rule out the possibility that SCs may receive transient innervation during development that has not yet been detected or reported in the literature. Transient neural-glial synapses have been detected in tissue cultures (e.g., Palacios-Prü et al., 1983) and in the demyelinating spinal cord (Soffer and Raine, 1980), as well as developing cortical neurons (Edmunds and Parnavelas, 1983).

A subset of SCs in the mature mammalian cochlea (Deiters' cells & Hensen's cells) receive innervation (Wright and Preston, 1976; Liberman et al., 1990; Nadol and Burgess, 1994; Burgess et al., 1997; Fechner et al., 1998, 2001). The synaptic specializations of these synapses are reported to consist of an accumulation of vesicles, both clear and dense core, on the presynaptic neural side and the thickening of pre- and postsynaptic membranes (Nadol and Burgess, 1994; Burgess et al., 1997). Synaptic bodies have never been reported. Our identification of a [^{3}H]thymidine-labeled cell with clear synaptic bodies is strongly suggestive of it being a labeled hair cell.

Our identification of new immature HCs in the mammalian vestibular epithelium 4 days after drug exposure is consistent with estimates of the time it takes for new HCs to be produced in regenerating and normal avian sensory epithelia. In avians, new auditory HCs first appear by 3–4 days after the onset of a damaging stimulus (Cotanche, 1987; Girod et al., 1989; Stone and Cotanche, 1992; Wang and Raphael, 1996; Stone et al., 1996; Stone and Rubel, 2000). The story is incomplete in avian vestibular tissues, partly as a consequence of the ongoing production of new SCs and HCs that occurs normally in this tissue (Jørgensen and Mathiesen, 1988; Roberson et al., 1992). However, it is not unreasonable to speculate that HCs might appear approximately 3 days after the onset of a damage stimulus in this tissue as well. This speculation is based on findings that SCs first enter S phase 16 hours after insult (Warchol and Corwin, 1996), and immature vestibular HCs are seen in the normal vestibular epithelium 2 days after S phase (Matsui et al., 2000).

Robust levels of new HC production by means of a mitotic pathway are seen in regenerating avian vestibular sensory epithelia (Weisleder and Rubel, 1993), whereas, cell proliferation in the mammalian vestibular epithelium is very limited (Lambert, 1994; Rubel et al., 1995; Tanyeri et al., 1995; Li and Forge, 1997; Zheng and Gao, 1997; Kuntz and Oesterle, 1998; Forge et al., 1998; Ogata et al., 1999). Only 2 of the 43 labeled cells examined by TEM appeared to be newly generated HCs on the basis of having synaptic specializations. Increased numbers of labeled cells with synaptic specializations may be seen with longer survival times. Our goal was not to exhaustively quantitate how many new cells with synaptic specializations are present but to show that some new cells have synaptic specializations. Future studies are needed to delineate the lifespan of the newly generated cells and to more further characterize their phenotypes.

One interpretation is that the labeled cells with synaptic specializations are not new cells but are damaged hair cells that will go on to die or maybe recover, the peculiarities of the nerve endings being a consequence of that damage. The ultrastructural characteristics of the labeled cells with synaptic specializations were carefully examined to assess this possibility. Ultrastructural features that are characteristic for dying cells were not detected. The cell shown in Figures 4 and 5 has clearly identifiable presynaptic bodies opposed to afferent terminals. The absence of features common to degenerating cells suggests that the labeled cell is newly generated, not a damaged HC that has re-entered the cell cycle. The labeled cell of Figures 2 and 3 has three primordial synaptic contacts with neural processes but presents a more mixed picture. Two ultrastructural features typically seen in damaged cells are seen in this cell (irregular invaginated nucleus with clumped chromatin and presence of a few primary lysosomes). However, the neural elements contacting this cell are clearly primordial in nature and indicative of developing neural contacts (Newman-Gage and Westrum, 1984; Kunkel et al., 1987; Vaughn, 1989). Furthermore, numerous polyribosomes are present within this cell, suggesting the absence of marked ribosomal lysis. It is conceivable that some newly generated cells may not live for long periods of time, similar to some olfactory neurons (Carr and Farbman, 1993) and the atypical cells in injured organ of Corti (Lenoir and Vago, 1996, 1997; Daudet et al., 1998). Such a phenomenon might explain the reported absence of newly generated cells in the lumenal layer of drug-damaged guinea pig utricular macula at long survival times (Rubel et al., 1995) or absence of cells double-labeled for calmodulin (a hair-cell marker) and BrdU in gerbil utricular macula allowed to survive 1–4 weeks after drug-induced damage (Ogata et al., 1999).

Production of new supporting cells in the mature mammalian vestibular SE

Earlier in vitro (Warchol et al., 1993; Lambert, 1994; Yamashita and Oesterle, 1995) and in vivo (Rubel et al., 1995; Tanyeri et al., 1995; Li and Forge, 1997; Kuntz and Oesterle, 1998; Ogata et al., 1999) studies reported the occurrence of new cells labeled with a cell proliferation marker in regions of the mammalian vestibular epithelium near the basement membrane. These cells have traditionally been considered to be SCs. In the normal mammalian vestibular epithelium, the location of the cell nucleus has played an important role in allowing the determination of cell type; nuclei located in the upper portion of the epithelium are traditionally regarded as belonging to HCs, and nuclei in the lower portion of the epithelium, adjacent to the basilar membrane, are considered to be SCs. After injury, the position of the cell nuclei in the epithelium becomes a much more tenuous indicator of cell type. For example, cells located near the M phase of the cell cycle are usually also located in the lumenal nuclear layer (Raphael, 1992; Katayama and Corwin, 1993; Tsue et al., 1994). Our ultrastructural analysis of mitotically labeled cells with basally located nuclei supports the conclusion that some of these cells are indeed SCs. However, some are clearly leukocytes. In addition, we located SC nuclei in the upper half of the epithelium. Hence, nuclear location is probably not a reliable indicator of cell type in vestibular macular epithelium after damage or in vitro, particularly at times when the epithelium is beginning to collapse.

Leukocytes within the SE

Leukocytes are recruited to sites of tissue injury and play a part in tissue repair. They secrete cytokines that stimulate the proliferation of numerous cell types, including some CNS glia (reviewed in Hamilton et al., 1993; Turpin and Lopez-Berestein, 1993). Several studies have suggested that leukocytes might respond to injuries in

inner ear epithelia. Increased leukocyte numbers are found in the mammalian cochlea after labyrinthine infection (Takahashi and Harris, 1988; Gloddek et al., 1991) and acoustic trauma (Fredelius and Rask-Andersen, 1990; Roberson and Rubel, 1994). Macrophages and other leukocytes are recruited to sites of HC lesions in cultured (Warchol, 1997) and in vivo avian inner ear sensory epithelia (Bhave et al., 1998). Leukocyte numbers increase at lesion sites before regenerative proliferation in HC epithelia (Jones and Corwin, 1993, 1996; Warchol, 1997; Bhave et al., 1998). The functional roles of leukocytes in the inner ear are unclear. They may secrete substances that are mitogenic for nearby SCs, thus initiating SC proliferation (Corwin et al., 1991). Two recent observations support this idea: (1) TNF-α, a macrophage secretory product, enhances proliferation of cultured vestibular SCs, and (2) dexamethasone, an anti-inflammatory drug that inhibits cytokine production by macrophages, reduces SC proliferation in cultured utricular macula after HC injury (Warchol, 1999).

There is little knowledge regarding the specific types of leukocytes that are recruited to sites of HC lesions and whether these subtypes release cytokines initiating cell proliferation. Previous studies support the existence of macrophages in axolotl lateral line organs (Jones and Corwin, 1993, 1996) and avian inner ear sensory epithelia (Warchol, 1997; Bhave et al., 1998). Macrophages (Bohne, 1971; Fredelius and Rask-Andersen, 1990; Roberson and Rubel, 1994; Vago et al., 1998) and monocytes were seen in the mammalian organ of Corti (Fredelius and Rask-Andersen, 1990). We report here the presence of macrophages, neutrophils, and lymphocytes in mammalian vestibular SE. We observed leukocytes in both normal and drug-damaged SE. A resident population of leukocytes normally resides in undamaged avian inner ear sensory epithelia (Warchol, 1997; Bhave et al., 1998). Our findings suggest that several leukocyte subtypes may reside normally in normal mammalian vestibular SE. However, we cannot rule out the possibility that the osmotic pump implantation resulted in leukocyte recruitment. Our findings also support the existence of several leukocyte subtypes in damaged ear epithelia, and studies examining functional roles of leukocytes within the damaged epithelium need to take this into consideration.

We observed proliferating leukocytes (macrophages and lymphocytes labeled with a mitotic tracer) within the mammalian SE. Hence, studies of mitotic tracer incorporation in inner ear sensory epithelia after experimental treatment need to take into account that a subset of the labeled cells seen within the epithelia are likely to be labeled immune cells or other nonsensory epithelial cells. Our findings are harmonious with previous reports of proliferating macrophages in cultured avian basilar papilla (Warchol, 1997) and mammalian organ of Corti (Roberson and Rubel, 1994; Vago et al., 1998). We also observed numerous labeled "active cells." The ultrastructural characteristics of these cells did not allow a definitive identification of cell type. They were suggestive, however, of their being immature immune elements, or possibly pericyte-like cells, or cells derived from fibroblasts. Small mononuclear cells approximately 8.0–10 μms in diameter, with scant cytoplasm that contains few cell organelles other than mitochondria, have been reported in human mammalian vestibular organs, in the intra- and subepithelial layers of the dark cell area in the semicircular canals and utricle (Masuda et al., 1997). Masuda and colleagues suggest that these cells may be T lymphocytes, as they observed small cells at the light microscope level in this region that stained with leukocyte common antigen (LCA) and UCHL-1.

Do hair cells re-enter the cell cycle after damage then die?

During the course of the study, we observed one [^{3}H]thymidine-labeled HC with ultrastructural features of a dying cell (multilobed electron-lucent nucleus, numerous lysosomes in the cytoplasm). Several neural elements were juxtaposed to the labeled cell. The [^{3}H]thymidine uptake by the HC might be the result of the following: (1) the cell's attempt to repair its DNA; (2) the HC's re-entry into the cell cycle pathway, which in turn triggers its subsequent entrance into an apoptotic pathway, leading to the death of the HC; or (3) the death of a newly generated HC. Possibilities one and three are unlikely. Numerous silver grains were detected over the nucleus of the cell, whereas only a small number of silver grains would be expected in a quiescent cell repairing its DNA. It is unlikely that this cell was a dying regenerated HC, because it was detected in a drug-damaged animal that was perfused with [^{3}H]thymidine for 3 days and killed 1 day later. Studies in rapidly regenerating avian inner ear sensory epithelia indicate it takes approximately 16 hours for a cell to enter S-phase after HC death/damage (Girod et al., 1989; Stone and Cotanche, 1994; Warchol and Corwin, 1996) and 2 days after S-phase until immature bundle formation is observed (Stone et al., 1996; Matsui et al., 2000; Stone and Rubel, 2000). Hence, in this cell, insufficient time had passed for the generation of a HC with a mature stereociliary bundle. Therefore, the second option presented above, that the labeled HC re-entered the cell cycle, passed into S phase (or farther), and subsequently entered an apoptotic pathway, seems most likely.

Hair cells are generally thought of as being effectively precluded from division and to reside in a state of terminal differentiation. However, there is growing evidence that, in pathologic conditions, many "terminally differentiated" cell types, particularly neuronal cell types, may attempt to re-enter the cell cycle and then default to an apoptotic-like pathway. This abortion of the cycle is thought to be involved in pathologic events such as Alzheimer's disease and other neurologic diseases (reviewed in Meikrantz and Schlegel, 1995; Evan and Littlewood, 1998; Raina et al., 1999, 2000; Nagy, 2000). Our findings suggest that HCs may show similar behavior, as part of an apoptotic-like response.

ACKNOWLEDGMENTS

The authors thank Sidya Ty and Judith Debel for excellent histologic work and assistance with figures; Glen MacDonald for assistance with digital photography and imaging techniques; Drs. Donald Born, Andrew Farr, Rémy Pujol, Michael Reidy, Rodney Schmidt, and Stephen Schwartz for assistance in interpreting photomicrographs and helpful discussions; and Dr. Alice Kuntz for help with the initial experiments.

LITERATURE CITED

Adler HJ, Raphael Y. 1996. New hair cells arise from supporting cell conversion in the acoustically damaged chick inner ear. Neurosci Lett 205:17–20.

Baird RA, Torres MA, Schuff NR. 1993. Hair cell regeneration in the bullfrog vestibular otolith organs following aminoglycoside toxicity. Hear Res 65:164–174.

Baird RA, Steyger PS, Schuff NR. 1996. Mitotic and nonmitotic hair cell regeneration in the bullfrog vestibular otolith organs. Ann N Y Acad Sci 781:59–70.

Baird RA, Burton MD, Lysakowski A, Fashena DS, Naeger RA. 2000. Hair cell recovery in mitotically blocked cultures of the bullfrog saccule. Proc Natl Acad Sci U S A 97:11722–11729.

Balak KJ, Corwin JT, Jones JE. 1990. Regenerated hair cells can originate from supporting cell progeny: evidence from phototoxicity and laser ablation experiments in the lateral line system. J Neurosci 10:2502–2512.

Bhave SA, Oesterle EC, Coltrera MD. 1998. Macrophage and microglia-like cells in the avian inner ear. J Comp Neurol 398:241–256.

Bohne B. 1971. Scar formation in the inner ear following acoustic injury: sequence of changes from early signs of damage to healed lesion. Thesis. St. Louis, Missouri: Washington University.

Burgess BJ, Adams JC, Nadol JB Jr. 1997. Morphologic evidence for innervation of Deiters' and Hensen's cells in the guinea pig. Hear Res 108:74–82.

Carr VM, Farbman AL. 1993. The dynamics of cell death in the olfactory epithelium. Exp Neurol 124:308–314.

Chardin S, Romand R. 1995. Regeneration and mammalian auditory hair cells. Science 267:707–711.

Corwin JT, Cotanche DA. 1988. Regeneration of sensory hair cells after acoustic trauma. Science 240:1772–1774.

Corwin JT, Jones JE, Katayama A, Kelley MW, Warchol ME. 1991. Hair cell regeneration: the identities of progenitor cells, potential triggers and instructive cues. Ciba Found Symp 1991;160:103–120.

Cotanche DA. 1987. Regeneration of hair cell stereociliary bundles in the chick cochlea following severe acoustic trauma. Hear Res 30:181–195.

Daudet N, Vago P, Ripoll C, Humbert G, Pujol R, Lenoir M. 1998. Characterization of atypical cells in the juvenile rat organ of Corti after aminoglycoside ototoxicity. J Comp Neurol 401:145–162.

Duckert LG, Rubel EW. 1990. Ultrastructural observations on regenerating hair cells in the chick basilar papilla. Hear Res 48:161–182.

Duckert LG, Rubel EW. 1993. Morphological correlates of functional recovery in the chicken inner ear after gentamycin treatment. J Comp Neurol 331:75–96.

Edmunds SM, Parnavelas JG. 1983. Presynaptic astrocytes in rat visual cortex. Brain Res 259:285–287.

Engström H. 1961. The innervation of the vestibular sensory cells. Acta Otolaryngnol Suppl (Stockh) 163:30–40.

Engström H, Bergström B, Rosenhall U. 1974. Vestibular sensory epithelia. Arch Otolaryngol 100:411–418.

Evan G, Littlewood T. 1998. A matter of life and cell death. Science 281:1317–1322.

Favre D, Sans A. 1977. Synaptogenesis of the efferent vestibular nerve endings of the cat: ultrastructural study. Arch Otorhinolaryngol 215: 183–186.

Favre D, Sans A. 1979. Embryonic and postnatal development of afferent innervation in cat vestibular receptors. Acta Otolaryngol 87:97–107.

Favre D, Dememes D, Sans A. 1986. Microtubule organization and synaptogenesis in the vestibular sensory cells. Dev Brain Res 25:137–142.

Fechner FP, Burgess BJ, Adams JC, Liberman MC, Nadol JB Jr. 1998. Dense innervation of Deiters' and Hensen's cells persists after chronic deefferentation of guinea pig cochleas. J Comp Neurol 400:299–309.

Fechner FP, Nadol JB Jr, Burgess BJ, Brown MC. 2001. Innervation of supporting cells in the apical turns of the guinea pig cochlea is from type II afferent fibers. J Comp Neurol 429:289–298.

Forge A, Li L, Corwin JT, Nevill G. 1993. Ultrastructural evidence for hair cell regeneration in the mammalian inner ear [see comments]. Science 259:1616–1619.

Forge A, Li L, Nevill G. 1998. Hair cell recovery in the vestibular sensory epithelia of mature guinea pigs. J Comp Neurol 397:69–88.

Fredelius L, Rask-Andersen H. 1990. The role of macrophages in the disposal of degeneration products within the organ of Corti after acoustic overstimulation. Acta Otolaryngol (Stockh) 109:76–82.

Gale JE, Meyers JR, Periasamy A, Corwin JT. 2000. Survival of bundleless hair cells and subsequent bundle replacement in the bullfrog's saccule. J Neurobiol 50:81–92.

Ginzberg RD, Gilula, NB. 1980. Synaptogenesis in the vestibular sensory epithelium of the chick embryo. J Neurocytol 9:405–424.

Girod DA, Duckert LG, Rubel EW. 1989. Possible precursors of regenerated hair cells in the avian cochlea following acoustic trauma. Hear Res 42:175–194.

Gloddek B, Ryan AF, Harris JP. 1991. Homing of lymphocytes to the inner ear. Acta Otolaryngol (Stockh) 111:1051–1059.

Hamilton DW. 1968. The calyceal synapse of type I vestibular hair cells. J Ultrastruct Res 23:98–114.

Hamilton TA, Ohmori Y, Narumi S, Tannenbaum CS, editors. 1993. Regulation of diversity of macrophage activation. Ann Arbor, Mich: CRC Press.

Jones JE, Corwin JT. 1993. Replacement of lateral line sensory organs during tail regeneration in salamanders: identification of progenitor cells and analysis of leukocyte activity. J Neurosci 13:1022–1034.

Jones JE, Corwin JT. 1996. Regeneration of sensory cells after laser ablation in the lateral line system: hair cell lineage and macrophage behavior revealed by time-lapse video microscopy. J Neurosci 16:649–662.

Jørgensen JM, Mathiesen C. 1988. The avian inner ear. Continuous production of hair cells in vestibular sensory organs, but not in the auditory papilla. Naturwissenschaften 75:319–320.

Katayama A, Corwin JT. 1993. Cochlear cytogenesis visualized through pulse labeling of chick embryos in culture. J Comp Neurol 333:28–40.

King DG, Kammlade N, Murphy J. 1982. A simple device to help re-embed thick plastic sections. Stain Technol 57:307–310.

Kirkegaard M, Jørgensen JM. 2000. Continuous hair cell turnover in the inner ear vestibular organs of a mammal, the Daubenton's bat (*Myotis daubentonii*). Naturwissenschaften 87:83–86.

Kirkegaard M, Jørgensen JM. 2001. The inner ear macular sensory epithelia of the Daubenton's bat. J Comp Neurol 438:433–444.

Kunkel DD, Westrum LE, Bakay RAE. 1987. Primordial synaptic structures and synaptogenesis in rat olfactory cortex. Synapse 1:191–201.

Kuntz AL, Oesterle EC. 1998. Transforming growth factor alpha with insulin stimulates cell proliferation in vivo in adult rat vestibular sensory epithelium. J Comp Neurol 399:413–423.

Lambert PR. 1994. Inner ear hair cell regeneration in a mammal: identification of a triggering factor. Laryngoscope 104:701–718.

Lambert PR, Gu R, Corwin JT. 1997. Analysis of small hair bundles in the utricles of mature guinea pigs. Am J Otol 18:637–643.

Lenoir M, Vago P. 1996. Morphological indications of hair cell neodifferentiation in the organ of Corti of amikacin treated rat pups. CR Acad Sci Paris 319:260–270.

Lenoir M, Vago P. 1997. Does the organ of Corti attempt to differentiate new hair cells after antibiotic intoxication in rat pups? Int J Dev Neurosci 15:487–495.

Li L, Forge A. 1997. Morphological evidence for supporting cell to hair cell conversion in the mammalian utricular macula. Int J Dev Neurosci 15:433–446.

Liberman C, Dodds LW, Pierce S. 1990. Afferent and efferent innervation of the cat cochlea; quantitative analysis with light and electron microscopy. J Comp Neurol 301:443–460.

Lopez I, Honrubia V, Lee SC, Schoeman G, Beykirch K. 1997. Quantification of the process of hair cell loss and recovery in the chinchilla crista ampullaris after gentamicin treatment. Int J Dev Neurosci 15:447–461.

Lopez I, Honrubia V, Lee SC, Li G, Beykirch K. 1998. Hair cell recovery in the chinchilla crista ampullaris after gentamicin treatment: a quantitative approach. Otolaryngol Head Neck Surg 119:255–262.

Lysakowski A. 1996. Synaptic organization of the crista ampullaris in vertebrates. New directions in vestibular research. Ann N Y Acad Sci 781:164–182.

Lysakowski A, Goldberg JM. 1997. A regional ultrastructural analysis of the cellular and synaptic architecture in the chinchilla cristae ampullares. J Comp Neurol 389:419–443.

Masuda M, Yamazaki K, Kanzaki J, Hosoda Y. 1997. Immunohistochemical and ultrastructural investigation of the human vestibular dark cell area: roles of subepithelial capillaries and T lymphocyte-melanophage interaction in an immune surveillance system. Anat Rec 249:153–162.

Matsui JI, Oesterle EC, Stone JS, Rubel EW. 2000. Characterization of damage and regeneration in cultured avian utricles. J Assoc Res Otolaryngol 1:46–63.

Mbiene JP, Favre D, Sans A. 1988. Early innervation and differentiation of hair cells in the vestibular epithelia of mouse embryos: SEM and TEM study. Anat Embryol (Berl) 177:331–340.

Meikrantz W, Schlegel R. 1995. Apoptosis and the cell cycle. J Cell Biochem 58:160–174.

Nadol JB Jr, Burgess BJ. 1994. Supranuclear efferent synapses on outer hair cells and Deiters' cells in the human organ of Corti. Hear Res 81:49–56.

Nagy Z. 2000. Cell cycle regulatory failure in neurones: causes and consequences. Neurobiol Aging 21:761–769.

Newman-Gage H, Westrum LE. 1984. Independent development of presynaptic specializations in olfactory cortex of the fetal rat. Cell Tissue Res 237:103–109.

Nordemar H. 1983. Embryogenesis of the inner ear. Acta Otolaryngol 96:1–8.

Oesterle EC, Cunningham DE, Westrum LE, Rubel EW. 2000. Ultrastructural analysis of proliferating cells in the in vivo rat utricular macula. Assoc Res Otolaryngol Abstr 23:162.

Ofsie MS, Hennig AK, Messana EP, Cotanche DA. 1997. Sound damage and gentamicin treatment produce different patterns of damage to the efferent innervation of the chick cochlea. Hear Res 113:207–223.

Ogata Y, Slepecky NB, Takahashi M. 1999. Study of the gerbil utricular macula following treatment with gentamicin, by use of bromodeoxyuridine and calmodulin immunohistochemical labelling. Hear Res 133:53–60.

Palacios-Prü EL, Mendoza RU, Palacios L. 1983. In vitro and in situ formation of neuronal-glia junctions. Exp Neurol 182:541–569.

Park JC, Hubel SB, Woods AD. 1987. Morphometric analysis and fine structure of the vestibular epithelium of aged C57BL/6Nnia mice. Hear Res 28:87–96.

Presson JC, Lanford PJ, Popper AN. 1996. Hair cell precursors are ultrastructurally indistinguishable from mature support cells in the ear of a postembryonic fish. Hear Res 100:10–20.

Raina AK, Monteiro MJ, Mcshea A, Smith MA. 1999. The role of cell cycle-mediated events in Alzheimer's disease. Int J Exp Pathol 80:71–76.

Raina AK, Zhu X, Rottkamp CA, Monteiro M, Takeda A, Smith, MA. 2000. Cyclin' toward dementia: cell cycle abnormalities and abortive oncogenesis in Alzheimer disease. J Neurosci Res 61:128–133.

Raphael Y. 1992. Evidence for supporting cell mitosis in response to acoustic trauma in the avian inner ear. J Neurocytol 21:663–671.

Roberson DW, Rubel EW. 1994. Cell division in the gerbil cochlea after acoustic trauma. Am J Otol 15:28–34.

Roberson DF, Weisleder P, Bohrer PS, Rubel EW. 1992. Ongoing production of sensory cells in the vestibular epithelium of the chick. Hear Res 57:166–174.

Roberson DW, Kreig CS, Rubel EW. 1996. Light microscopic evidence that direct transdifferentiation gives rise to new hair cells in regenerating avian auditory epithelium. Audit Neurosci 2:195–205.

Rubel EW, Dew LA, Roberson DW. 1995. Mammalian vestibular hair cell regeneration [letter; comment]. Science 267:701–707.

Ross MD. 1997. Morphological evidence for local microcircuits in rat vestibular maculae. J Comp Neurol 379:333–346.

Rüsch A, Lysakowski A, Eatock RA. 1998. Postnatal development of type I and type II hair cells in the mouse utricle: acquisition of voltage-gated conductances and differentiated morphology. J Neurosci 18:7487–7501.

Ryals BM, Rubel EW. 1988. Hair cell regeneration after acoustic trauma in adult Coturnix quail. Science 240:1774–1776.

Ryals BM, Westbrook EW. 1994. TEM analysis of neural terminals on autoradiographically identified regenerated hair cells. Hear Res 72:81–88.

Ryals BM, Westbrook EW, Stoots S, Spencer RF. 1992. Changes in the acoustic nerve after hair cell regeneration. Exp Neurol 115:18–22.

Sánchez-Fernández JM, Rivera-Pomar JM. 1983. A study of the development of utricular and saccular maculae in man and rat. Am J Otol 5:44–49.

Sans A, Dechesne CJ. 1987. Afferent nerve ending development and synaptogenesis in the vestibular epithelium of human fetuses. Hear Res 28:65–72.

Sobkowicz HM. 1992. The development of innervation in the organ of Corti. In: Romand R, editor. Development of auditory and vestibular systems 2. Amsterdam: Elsevier Science Publishers. p 59–100.

Sobkowicz HM, August BK, Slapnick SM. 1992. Epithelial repair following mechanical injury of the developing organ of Corti in culture: an electron microscopic and autoradiographic study. Exp Neurol 115:44–49.

Sobkowicz HM, August BK, Slapnick SM. 1996. Post-traumatic survival and recovery of the auditory sensory cells in culture. Acta Otolaryngol 116:257–262.

Sobkowicz HM, August BK, Slapnick SM. 1997. Cellular interactions as a response to injury in the organ of Corti in culture. Int J Dev Neurosci 15:463–485.

Soffer D, Raine CS. 1980. Morphological analysis of axoglial membrane in the demyelinated central nervous system. Brain Res 186:301–313.

Steyger PS, Burton M, Hawkins JR, Schuff NR, Baird RA. 1997. Calbindin and parvalbumin are early markers of non-mitotically regenerating hair cells in the bullfrog vestibular otolith organs. Int J Dev Neurosci 15:417–432.

Stone JS, Cotanche DA. 1992. Synchronization of hair cell regeneration in the chick cochlea following noise damage. J Cell Sci 102:671–680.

Stone JS, Cotanche DA. 1994. Identification of the timing of S phase and the patterns of cell proliferation during hair cell regeneration in the chick cochlea. J Comp Neurol 341:50–67.

Stone JS, Rubel EW. 2000. Temporal, spatial, and morphologic features of hair cell regeneration in the avian basilar papilla J Comp Neurol 417:1–16.

Stone JS, Leaño SG, Baker LP, Rubel EW. 1996. Hair cell differentiation in chick cochlear epithelium after aminoglycoside toxicity: in vivo and in vitro observations. J Neurosci 16:6157–6174.

Takahashi M, Harris JP. 1988. Anatomic distribution and localization of immunocompetant cells in the normal mouse endolymphatic sac. Acta Otolaryngol 106:409–416.

Takumida M, Miyawaki H, Harada Y. 1995. Cytoskeletal organization of the vestibular sensory epithelia. Acta Otolaryngol (Stockh) 519:66–70.

Tanyeri H, Lopez I, Honrubia V. 1995. Histological evidence for hair cell regeneration after ototoxic cell destruction with local application of gentamicin in the chinchilla crista ampullaris. Hear Res 89:194–202.

Tsue TT, Watling DL, Weisleder P, Coltrera MD, Rubel EW. 1994. Identification of hair cell progenitors and intermitotic migration of their nuclei in the normal and regenerating avian inner ear. J Neurosci 14:140–152.

Turpin JA, Lopez-Berestein G. 1993. Differentiation, maturation, and activation of monocytes and macrophages: functional activity is controlled by a continuum of maturation. In: Lopez-Berestein G, Klostergaard J, editors. Mononuclear phagocytes in cell biology. Ann Arbor, Mich: CRC Press. p 72–99.

Vago P, Humbert G, Lenoir M. 1998. Amikacin intoxication induces apoptosis and cell proliferation in rat organ of Corti. Neuroreport 9:431–436.

Vaughn JE. 1989. Review: fine structure of synaptogenesis in the vertebrate central nervous system. Synapse 3:255–285.

Wang Y, Raphael Y. 1996. Re-innervation patterns of chick auditory sensory epithelium after acoustic overstimulation. Hear Res 97:11–18.

Warchol ME. 1997. Macrophage activity in organ cultures of the avian cochlea: demonstration of a resident population and recruitment to sites of hair cell lesions. J Neurobiol 33:724–734.

Warchol ME. 1999. Immune cytokines and dexamethasone influence sensory regeneration in the avian vestibular periphery. J Neurocytol 28: 889–900.

Warchol ME, Corwin JT. 1996. Regenerative proliferation in organ cultures of the avian cochlea: identification of the initial progenitors and determination of the latency of the proliferative response. J Neurosci 16:5466–5477.

Warchol ME, Lambert PR, Goldstein BJ, Forge A, Corwin JT. 1993. Regenerative proliferation in inner ear sensory epithelia from adult guinea pigs and humans. Science 259:1619–1622.

Weisleder P, Rubel EW. 1993. Hair cell regeneration after streptomycin toxicity in the avian vestibular epithelium. J Comp Neurol 331:97–110.

Wersäll J. 1956. Studies on the structure and innervation of the sensory epithelium of the cristae ampullares in the guinea pig. A light and electron microscopic investigation. Acta Otolaryngol Suppl 126:1–85.

Westrum LE, Gray EG, Burgoyne RD, Barron J. 1983. Synaptic development and microtubule organization. Cell Tissue Res 231:93–102.

Westrum LE, Cunningham DE, Anderson NL, Rubel EW. 1999. Deafferentation and reinnervation of chick auditory hair cells after gentamicin damage: an ultrastructural study. Assoc Res Otolaryngol Abstr 22: 127–128.

Wright CG, Preston RE. 1976. Efferent nerve fibers associated with the outermost supporting cells of the organ of Corti in the guinea pig. Acta Otolaryngol 82:41–47.

Yamashita H, Oesterle EC. 1995. Induction of cell proliferation in mammalian inner ear sensory epithelia by transforming growth factor-alpha and epidermal growth factor. Proc Natl Acad Sci U S A 92:3152–3155.

Zheng JL, Gao W-Q. 1997. Analysis of rat vestibular hair cell development and regeneration using calretinin as an early marker. J Neurosci 17:8270–8282.

Zheng JL, Helbig C, Gao W-Q. 1997. Induction of cell proliferation by fibroblast and insulin-like growth factors in pure rat inner ear epithelial cell cultures. J Neurosci 17:216–226.

Zheng JL, Frantz G, Lewis AK, Sliwkowski M, Gao W-Q. 1999. Heregulin enhances regenerative proliferation in postnatal rat utricular sensory epithelium after ototoxic damage. J Neurocytol 28:901–912.